Nonparametric Bandits Leveraging Informational Externalities to Learn the Demand Curve

Ian N. Weaver
National University of Singapore Business School; i.weaver@nus.edu.sg

Vineet Kumar
Yale School of Management; vineet.kumar@yale.edu

Lalit Jain
Foster School of Business, University of Washington; lalitj@uw.edu

We propose a novel, theory-based approach to the reinforcement learning problem of maximizing profits when faced with an unknown demand curve. Our method, grounded in multi-armed bandits, balances exploration and exploitation to maximize rewards across various options (arms). Traditional Gaussian process bandits capture one informational externality in price experimentation — correlation of rewards through an underlying demand curve. We expand on this by incorporating a second externality, monotonicity, into the Gaussian process bandit framework by providing monotonic versions of both the GP-UCB and GP-TS algorithms. This incorporation limits unnecessary exploration (reducing experimentation) and outperforms benchmarks by enhancing profitability. Our approach can also complement methods such as partial identification. Furthermore, we present algorithm variants that address heteroscedasticity in purchase data noise. Across a broad range of demand distributions and price sets, our algorithm significantly increased profits, especially for willingness-to-pay distributions where the optimal price is low (among the set of prices considered). In every simulation setting, our algorithm consistently achieved over 95% of the optimal profits.

Key words: Multi-armed Bandits, Reinforcement Learning, Pricing

1. Introduction

We propose a new method based on reinforcement learning using multi-armed bandits (MABs) to efficiently learn an unknown demand curve. Our algorithm is a nonparametric method based on Gaussian process Thompson sampling that incorporates microeconomic theory to converge towards optimal pricing and profits, with significantly less experimentation required than current methods. We use weak restrictions on the monotonicity of demand, which creates an informational externality between the outcomes of arms in the MAB. Our method exploits this informational externality to achieve higher profitability, with the same level of experimentation as extant methods. The learned demand curve is also guaranteed to satisfy monotonicity criteria based on economic theory. The proposed method has several other advantages relative to state-of-the-art approaches, and can also be

used in a complementary manner with recent approaches like partial identification (Misra et al. 2019).

In practice, the demand curve is only known in the price range that an established product is sold, and unknown elsewhere. Pricing mistakes are greatest for new products that differ most from past products (Huang et al. 2022). Consider the case of the Atlanta Falcons, who in 2016 announced they would be dramatically slashing concessions to untested prices to improve brand equity. When asked how they projected the volume of sales to change, the CEO of the ownership group of the Falcons, Steve Cannon, replied, "It could be a 10 percent bump, it could be a 30 percent bump, who knows."[1] The next season sales volume for food rose 50%.[2] Even with a sophisticated marketing team, there is no perfect substitute for price experimentation about a particular product. Overall, McKinsey estimates that "30 percent of the thousands of pricing decisions companies make every year fail to deliver the best price."[3]

Knowledge of the demand curve is also a primary starting point for managers to implement pricing, promotion, and distribution strategies. Firms experiment often to learn the demand curve using trial and error (Furman and Simcoe 2015). Even in categories that are well known, demand can undergo significant changes over time. To learn demand at different price points, a simple approach is to use a balanced experiment (also called A/B testing) randomly allocating consumers across a set of different prices. However, firms across a wide range of industries are reluctant to do much price experimentation (Ariely 2010), as managers worry that price experimentation can confuse or alter consumers' expectations for uncertain gains. Managers often do not run experiments long enough, making detecting effects difficult (Hanssens and Pauwels 2016).

These factors imply that a method which can identify and learn the critical part of the demand curve efficiently using minimal experimentation can be quite valuable in consequently identifying the optimal price points for products. It is noteworthy that pricing differs from advertising, for which companies are more willing to experiment (Pfeffer and Sutton 2006, Sahni and Nair 2020, Huang et al. 2018, Simester et al. 2009). The pricing

[1] https://www.ajc.com/sports/the-economics-the-falcons-new-cheap-stadium-food/8xvH1bAYTewjU2KQoc5HyN/

[2] https://www.washingtonpost.com/sports/2019/03/06/were-evangelists-this-why-atlanta-falcons-are-selling-hot-dogs/

[3] https://www.mckinsey.com/business-functions/growth-marketing-and-sales/our-insights/using-big-data-to-make-better-pricing-decisions

problem is particularly suited to MABs which simultaneously learn while earning, avoiding the wasteful explorations using A/B testing. They deal with the classic trade-off between *exploitation* (current payoff) and *exploration* (learning additional information) as the agent tries to maximize their rewards over some horizon.

The core ideas in this paper expand on canonical bandits by leveraging two distinct but related sources of *informational externalities* across arms (prices). First, we know that demand at closer price points is more likely to be similar compared to demand at more distant price points. This feature of the pricing problem, which we term an information externality, implies that knowing the demand at a focal price point helps in learning about demand not only at that price, but also at other price points. Such learning is more likely to be greater for prices close to the focal price, and less for prices further away from it. The second informational externality is the characterization that aggregate demand curves are monotonic, consistent with microeconomic theory. Thus, the quantity demanded at a focal price must be *weakly lower* than the demand at all prices lower than the focal price. Incorporating these related sources of informational externality potentially helps us learn demand more efficiently and accurately, and forms the focus of this paper. We also explore whether the two informational externalities are substitutes, or whether they can act together in a complementary manner to improve performance.

Our method offers several advantages relative to extand methods for optimal pricing under unknown demand. The primary advantage is efficiency in optimal pricing by learning demand in a flexible nonparametric manner when the firm has no well-defined prior information about demand. If a firm is willing to undertake adaptive experimentation to learn demand, and wants to minimize the cost of experimentation, our method helps the firm achieve a higher profitability than current approaches across a robust range of underlying distributions of consumer valuation (willingness-to-pay). A second advantage is that the method offers a guaranteed way to incorporate theoretical knowledge into reinforcement learning problems. It can be applied to any vertical quality-like attribute, not just prices. More broadly, other domain-specific restrictions on demand based on prior conceptual knowledge can be incorporated into this framework. CHECK AE / SE Third, our method provides an estimate of uncertainty, along with point estimates of the demand curve. In fact, the entire posterior distribution can be obtained to provide a complete characterization of uncertainty around the learned demand curve. Fourth, there is little

to no human judgment required. Unlike most typical RL models, hyperparameter tuning is automatic, and the method is computationally tractable, allowing the bandit to run in real time. Fifth, an important aspect is that we do not require any knowledge about the market or consumer characteristics, unlike partial identification approaches like UCB-PI, which requires some knowledge of a consumer's segment membership (Misra et al. 2019). Our method can in fact be used in conjunction with partial identification.

Our method uses nonparametric reinforcement learning (RL) with simultaneous learning and earning, and is most appropriately situated in the class of other nonparametric RL models. In terms of algorithms for choosing arms, the Upper Confidence Bound (UCB) and Thompson sampling (TS) form the underlying set of methods that are commonly used in RL. The UCB algorithm (Auer 2002, Auer et al. 2002) is designed to explore the arms with higher payoffs, but also arms that have been less explored, with the idea that greater uncertainty implies greater potential rewards. The TS approach involves a Bayesian updating of the rewards distribution corresponding to each of the arms as they are played (Thompson 1933). Arms are chosen probabilistically, with arms that have a higher mean more likely to be chosen. TS is a stochastic approach, whereas UCB is deterministic.

Whereas the above methods choose arms, in the baseline algorithms above, the rewards across arms are independent. To incorporate dependence in rewards across arms, Gaussian processes (GP) have been used with both UCB and TS classes of RL algorithms. These first model a GP on the data (arm, rewards) and provide the ability to learn a more general reward function, as compared to learning about rewards corresponding to specific arms. A major challenge in using GPs for pricing problems is that we may obtain non-monotonic demand functions that are not consistent with economic theory. This issue is exacerbated by the fact that a GP models the entire demand distribution, meaning particularly noisy data at one price could affect the estimated demand at another price. Therefore, a method that can obtain monotonic demand curves from a GP is highly valuable; the challenge, however, is that specifying monotonicity in a GP is not trivial.

We propose a model that uses ideas from economic theory to guide the reinforcement learning process, by enforcing monotonicity on nonparametric bandits. More generally, this method can be easily adapted to any bandit situation where the underlying data has a vertical attribute.

Move to abstract, repetitive here. Our method provides a practical, quick, implementable algorithm with minimal assumptions or human judgment, which outperforms a wide range of benchmarks. The method is nonparametric, implying it does not depend on a restrictive (parametrized) model of what a demand curve should look like.

We specify monotonicity by building up a function interpolating its value from the sum of its derivatives at nearby points. Our method relies on the crucial foundation that the derivative of a GP is also a GP. For decreasing functions, the first derivative is always negative at every point. We leverage the idea that sign restrictions are easy to impose relative to shape restrictions like monotonicity. We are able to then impose sign restrictions in a different GP space (the space of derivative GPs) than the demand GP. Thus, we can restrict the first derivative of demand to be negative, which leads to our method drawing only monotonic demand curves from the GP.

There are a few main contributions made here. To researchers and practitioners, we provide a method that builds upon Gaussian process bandits to account for economic theory imposing the general property that demands curves are downward sloping. We specify an algorithm that efficiently obtains only monotonic, downward-sloping demand curves throughout the experimentation process. Our approach results in significantly higher profits relative to state-of-the-art methods in the MAB literature while having a lower variance between trials. The increase in efficiency means that a larger number of prices can be included in the consideration set. These are important managerial considerations, given the reluctance to do pricing experiments. More broadly, in other situations where data has some general known form a priori, our approach shows how such constraints can be combined with the flexibility of nonparametric bandits to improve empirical performance.

We compare our approach to several state-of-the-art benchmark methods. In simulations across a range of settings, our proposed algorithm outperforms these benchmarks. We found that our algorithm gained higher expected total profits than UCB, TS, GP-UCB, and GP-TS benchmarks. Averaged across three main simulation settings, we found that incorporating monotonicity into GP-UCB and GP-TS consistently increased profits by 10-26% after 500 consumers and 4-8% after 2500 consumers, regardless of the price set granularity. There was, however, substantial heterogeneity in the results depending on the underlying distribution, with the biggest boost occurring for distributions where the

optimal price was low within the price set. The reason is that benchmarks tend to over-explore higher prices as a result of the increasing scaling factor of the potential reward as the price increases. Our algorithm, in contrast, leverages monotonicity to limit over-exploration of higher prices, leading to more consistent results: over 95% of the optimal profits in every scenario tested.

2. Literature Review

Our research is related to several streams detailed below. The setting features pricing experimentation and learning over time, which is an active area of research across marketing, operations research, economics and computer science.

Demand Learning

Studies in marketing and economics typically make strong assumptions about the information that a firm has regarding product demand. The strongest assumption used is that the firm can make pricing decisions based on knowing the demand curve (or WTP) (Oren et al. 1982, Rao and Bass 1985, Tirole 1988). A generalization of this assumption is that firms know the demand only up to a parameter, used in some of the earlier works on learning demand through price experimentation (Aghion et al. 1991, Rothschild 1974). Typically, a consumer utility function is specified in terms of product characteristics, price, and advertising, and preference parameters are estimated from data (Zhang and Chung 2020, Jindal et al. 2020, Huang et al. 2022). However, all these models predetermine the shape of the demand curve, and cannot incorporate all possible demand curves. Nonparametric approaches are the gold standard, and have been used to account for state changes between periods, but are often simplified substantially (e.g. having two periods) to ensure analytical tractability (Bergemann and Schlag 2008, Handel and Misra 2015). This stream typically does not consider learning through active experimentation, which is the focus of multi-armed bandits stream below.

Multi-armed Bandits

Multi-armed bandit (MAB) methods are an active learning approach based on Reinforcement Learning and are used across many fields, with business applications in advertising (Schwartz et al. 2017), website optimization (Hill et al. 2017, Hauser et al. 2009), and recommendation systems (Kawale et al. 2015). Two fundamental arm selection algorithms (or decision rules) that form the foundation for MAB methods are (a) Upper Confidence

Bounds (UCB), based on Auer et al. (2002), which is a deterministic and (b) Thompson sampling (TS), based on Thompson (1933), a stochastic approach.

Wang et al. (2021), Chen et al. (2019), Lei et al. (2014), Miao and Wang (2024), Cheshire et al. (2020), Guntuboyina and Sen (2018), Chatterjee and Sen (2021)

Several previous works have explored dynamic pricing with non-parametric demand assumptions. These often enforce conditions like smoothness or unimodality, and then approximate the demand using locally parametric functions, such as polynomials Wang et al. (2021). However, the resulting algorithms depend heavily on these specific choices. In contrast, our approach imposes no constraints beyond the economically motivated monotonic shape constraint. Any further restrictions arise naturally from the chosen kernel (e.g., RBF or Matern), offering greater flexibility for practitioners hesitant to make strong assumptions.

While shape constraints have been considered in other contexts, their application to dynamic pricing and reward maximization remains limited. Thresholding bandits aim to find the arm closest to a given threshold, assuming monotonic arm rewards, but do not focus on maximizing rewards Cheshire et al. (2020). Other works primarily address the estimation problem Guntuboyina and Sen (2018), or consider contextual settings with monotonic mean distributions across arms Chatterjee and Sen (2021). These approaches, while valuable, do not directly translate to our dynamic pricing problem with a focus on reward maximization under shape constraints.

A separate line of work incorporates inventory constraints into dynamic pricing models Lei et al. (2014), Chen et al. (2019), Miao and Wang (2024). These studies often introduce constraints on revenue or utilize exploration phases that involve significant price fluctuations, which may not be feasible in practice. Furthermore, their solutions are typically driven by the characterization of the optimal posted price, differing from our approach.

However, traditional bandit methods typically only model rewards for individual arms, but not any dependencies across arms. In pricing applications, this independence ignores the information from the underlying demand curve, which we term as informational externalities. Recent research below has tried to develop methods to address this issue.

Gaussian Processes and Bandits: Gaussian Processes (GPs) are well-regarded as a highly flexible nonparametric method for modeling unknown functions (Srinivas et al. 2009). In

particular, GPs provide a principled approach to allowing dependencies across arms, without restricting the functional form. They have recently been used with multi-armed bandits by combining GPs along with a decision rule like UCB or Thompson sampling (TS) by Chowdhury and Gopalan (2017), who evaluate the theoretical and empirical performance of GP-UCB and GP-TS.

More specifically, a closely related paper by Ringbeck and Huchzermeier (2019) uses GP-TS for a multi-product pricing problem. The GP is modeled here at a demand level, which is important for two reasons. First, it allows them to model demand-level inventory constraints in a multi-product setting, and second, it allows for a separation of the learning problem (at demand level) from the rewards optimization (reward is the product of demand and price). Leveraging the first informational externality, they find that GP-TS improves performance over TS. However, much is not known about the conditions (e.g. the number of arms or WTP distribution) under which the informational externality modeled by GP-TS is important, with a material impact on profit outcomes. Our main focus here is on incorporating monotonicity of demand curves, a theory-based restriction that forms the second informational externality, into GP-TS and GP-UCB models, and evaluating the resulting models.

There are other approaches to rule out dominated prices (arms) in pricing bandits. One particularly notable contribution incorporating knowledge into bandits is the partial identification method (Misra et al. 2019), which does not rely on dependency across arms. Partial identification formalizes the notion that the rewards from a specific arm (price) can be dominated by another arm, and critically relies on the availability of highly informative segmentation data to obtain demand bounds for the segment. The demand bounds are then aggregated across all segments to obtain the corresponding aggregated rewards bounds for each price arm. Dominated prices are eliminated if the upper bound for one price is lower than the lower bound for a different price. In contrast, our algorithm does not need information on segmentation to leverage the gains from the monotonicity assumption. As the mechanisms across papers are different, it is possible to use partial identification as a complement to our approach to create a hybrid.

3. Pricing Problem and Simple Example

3.1. Pricing Problem

This paper addresses the pricing problem faced by a firm aiming to maximize cumulative profits while experimenting under an unknown demand curve. Potential buyers (consumers)

arrive sequentially and are presented with a price selected by the firm. Each consumer then decides whether to purchase a single unit or not (in line with Misra et al. (2019), we focus on discrete choice purchases), depending on whether the offered price is below or above their willingness to pay (WTP).[4] For each consumer, the reward (profit) received by the firm equals the price minus the cost if the consumer makes a purchase and zero otherwise.

Overall, the firm must make two key decisions. First is the selection of the set of prices to be tested in the experiment—this is assumed to be exogenous, although in our simulations we test multiple price sets with varying granularities to guide firms in this decision. Second, the firm is allowed to periodically adjust the price shown to an incoming consumer based on limited past purchase decisions obtained during the pricing experiment. This paper focuses on designing an algorithm that selects prices (from the price set) throughout the experiment to maximize profits. The algorithms considered belong to a class known as multi-armed bandits (MABs), described in Section 4.

We consider a few additional assumptions in this pricing problem. First, consumers are randomly drawn from a population with a stable WTP distribution of valuations. Second, consumers are short-lived, and the overall distribution of price expectations remains unaffected by the experimentation. These assumptions are typical in field experiments and necessary for the results to be applicable once the experiment has ended.[5] Third, we assume the firm operates as a single-product monopolist.[6] Fourth, the firm seeks to set a single optimal price, meaning it does not engage in price discrimination and does not consider inventory or other factors (Besbes and Zeevi 2009, Ferreira et al. 2018, Ringbeck and Huchzermeier 2019, Misra et al. 2019).[7] Finally, given the pace at which prices must be adjusted for efficient experimentation, our algorithms are suited to the online domain rather than physical stores.

[4] The population of consumers has a population-level distribution of WTP, which corresponds directly to the demand curve.

[5] This excludes dynamic situations where consumers may change over time or where current decisions are heavily influenced by future expectations. Such cases include strategic consumers (Nair 2007), learning (Erdem and Keane 1996, Yu et al. 2016), and stockpiling (Ching and Osborne 2020, Hendel and Nevo 2006). These assumptions are often implicit in field experiments, such as in the advertising literature (Hoban and Bucklin 2015, Lambrecht et al. 2018, Gordon et al. 2019). For instance, if strategic consumers believe that a firm offering discounts is experimenting and may discount further later, the observed treatment effect may not accurately reflect reality.

[6] This assumption can be relaxed; the results will hold as long as the algorithm is deployed in a stable environment where (1) competitors do not change prices strategically in response to real-time changes and (2) firms are unconcerned with potential future competitors (Rubel 2013).

[7] Inventory constraints are relevant when stock is limited, as in clothing. When products are constrained, it may be preferable to forgo selling to one consumer to sell to another with a higher WTP. For products without production constraints, such as a Netflix subscription, this issue does not arise.

3.2. Simple Pricing Experiment Example

In this section, we discuss a simple example of a balanced pricing experiment. This example helps illustrate why existing bandit algorithms may perform poorly for certain underlying WTP distributions, providing a setting where our algorithm can greatly increase performance.

Let us consider an example where a firm is selling a product that each consumer can purchase only one unit. Let the true, unknown demand curve be $D(p) = 1 - p$, the prices tested be $P = \{0.1, 0.3, 0.5, 0.7, 0.9\}$, and the costs be zero. The firm tests each price 100 times, and the results of the demand learning and profit learning are shown in Figure 1. Figure 1a) shows the sample mean demand at the prices tested (blue dots), along with their corresponding 95% credible intervals,[8] while Figure 1b) shows the sample mean profit at the prices tested (red dots), along with their corresponding 95% credible intervals. The grey dotted lines represent the true demand curve and true profit curve, respectively.

Figure 1 Demand and Profit Learning for a Balanced Experiment

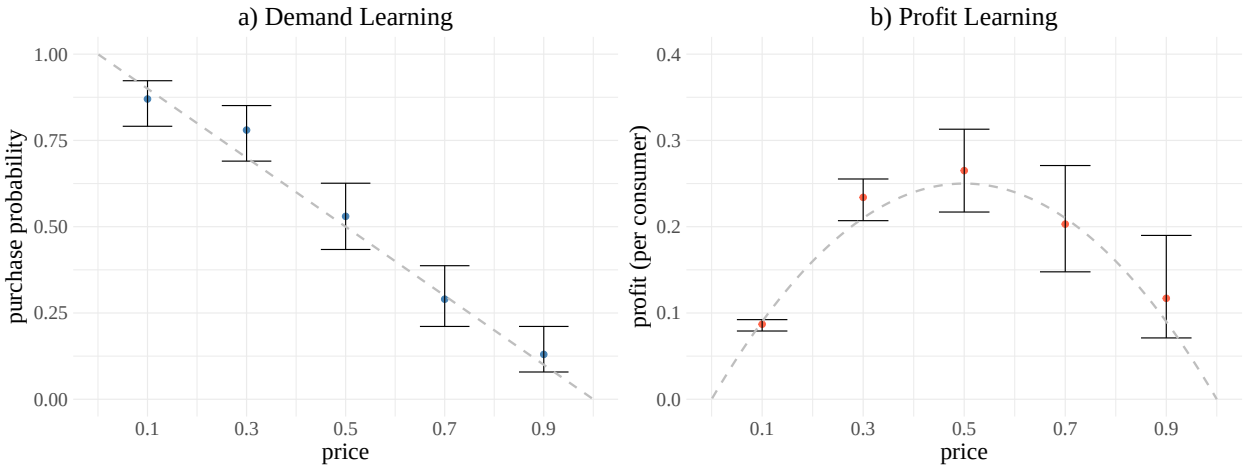

Notes. Results of a single balanced experiment where each of the prices $\{0.1, 0.3, 0.5, 0.7, 0.9\}$ was tested 100 times with a true unknown demand of $D(p) = 1 - p$. Figure a) shows the mean and 95% credible intervals for purchase probability at each price tested — the dotted grey line shows the true purchase probability. Figure b) shows the mean and 95% credible intervals for profit at each price tested — the dotted grey line shows the true expected profit.

This figure illustrates a crucial phenomenon. While the credible intervals at the demand level are roughly the same size,[9] at the profit level, they vary greatly and increase with price (as the profit intervals are obtained by scaling the demand intervals by price). In the pricing problem, learning happens at the demand level (whether a purchase is made

[8] Credible intervals are calculated by assuming a binomial prior.

[9] There are small differences, as discussed in Appendix EC.8.

or not), but determining the optimal price happens at the profit level. This means that the difficulty of the optimal pricing problem depends on where the optimal price is located among the set of prices being tested. If the optimal price is high, the problem is simple, as learning that low prices (with small profit intervals) are suboptimal is not a difficult task. However, if the optimal price is low, learning that high prices (with large profit intervals) are suboptimal is a much more difficult task, requiring a larger number of consumer purchase decisions. Overall, this leads to poorer algorithmic performance when the optimal price is low compared to when the optimal price is high.

This insight provides the mechanism by which incorporating monotonicity can lead to an increase in performance. This is because incorporating monotonicity rules out any demand curve with a region where demand increases as price increases. This allows for a reduction in the space of possible demand curves and thus in the demand intervals. In particular, this effect is magnified by the scaling effect, so that even a moderate decrease in the demand intervals can have large effects on reducing the profit intervals at high prices.

4. Model Preliminaries

4.1. MAB Components

This section formally introduces multi-armed bandits (MABs) and their application to the pricing problem. Notably, all MABs have three components: actions, rewards, and a policy.

The first component — *actions* — refers to the set of prices from which the firm can choose. Prior to the experiment, the firm selects a finite set of K ordered prices $P = \{p_1, \ldots, p_K\}$, where $p_1 < p_2 < \cdots < p_K$, and prices are scaled so that $0 \leq p_k \leq 1$.[10] While this paper does not explicitly model how to choose the set of prices, the general trade-off is that learning is easier with fewer prices, but a higher optimum is possible when more prices are considered. The results section provides general guidelines for how to pick the set of prices. Once P is chosen, at each time-step t of the experiment, the firm chooses a price p_k from P.

The second component — *rewards* — refers to the profits that a firm makes at each purchase opportunity. The firm faces an unknown true demand $D(p)$, and the true profit function is given by $\pi(p) = pD(p)$. We assume variable costs are zero, though the model can easily accommodate such costs.[11] The true profit is not observed; instead, the firm

[10] With unscaled prices $\{\widetilde{p_1}, \ldots, \widetilde{p_K}\}$, the set of scaled prices can be created by dividing any price by the largest price in the set, i.e., $p_k = \widetilde{p_k}/\widetilde{p_K}$.

[11] Simply, the reward obtained from a potential consumer who purchases is the price charged minus the cost.

Table 1 Summary of Bandit Notation

Notation	Description	Formula
Ψ	Policy for dynamic pricing (i.e., decision rule)	Depends on algorithm
k	Action index from the set of K actions	$k \in \{1, 2, ..., K\}$
t	Time-step: denotes the t-th consumer of the price experiment	
P	Set of prices to be tested	
p_k	Scaled price corresponding to action k	$p_k \in P = \{p_1, ..., p_K\}$ where $0 \leq p_k \leq 1 \; \forall p_k$
n_{kt}	Number of times price p_k has been chosen through time t	
s_{kt}	Number of purchases at price p_k through time t	
H_t	History from past t rounds of experiment	$H_t = \{S_t = (s_{1t}, ..., s_{Kt}), N_t = (n_{1t}, ..., n_{Kt})\}$
k_t	Action chosen at time t	$k_t = \Psi(P, H_{t-1})$
$D(p_k)$	Demand at price p_k	
y_{kt}	Purchase rate through time t of price p_k	$y_{kt} = s_{kt}/n_{kt}$
$\bar{\pi}_{kt}$	Mean profit through time t of price p_k	$\bar{\pi}_{kt} = p_{kt}(s_{kt}/n_{kt})$
π_{k_t}	Profit realized when price p_k was tested in time period t	

observes noisy realizations of profits corresponding to each price p_k. Considering the data at each price separately, we define n_{kt} to be the number of times that price p_k (arm k) has been chosen through time t, and s_{kt} to be the cumulative number of purchases for action k through time t. The observed purchase rate through time t for price p_k is simply $y_{kt} = \frac{s_{kt}}{n_{kt}}$. Accordingly, the mean profit for a price p_k at time t is $\bar{\pi}_{kt} = p_k \left(\frac{s_{kt}}{n_{kt}} \right)$.

The final component — a *policy* — denoted by Ψ, is a decision-making rule that picks an action or price in each round using the history from past rounds. In this situation, the history can be written as $H_t = \{S_t = (s_{1t}, \ldots, s_{Kt}), N_t = (n_{1t}, \ldots, n_{Kt})\}$. Formally, in round t, the policy picks a price using the history from the past $(t-1)$ rounds: $p_{k_t} = \Psi(P, H_{t-1})$. What distinguishes various MAB algorithms is how this policy is defined. For a typical randomized experiment, the policy can be defined as an equal probability across all arms, completely ignoring history. A summary of the notation is given in Table 1.

4.2. Performance Metrics

To assess the performance of our proposed algorithm, we need to compare it to other bandit algorithms. This is equivalent to a comparison of policies, as only the policy Ψ depends on the algorithm, while the price set and arm rewards are common across algorithms.

Among the various performance metrics in the bandit literature, the most common is regret, which is defined as the difference between rewards under full knowledge (always

playing the optimal price) and the expected rewards from the policy in question (Lai and Robbins 1985). Formally, the cumulative regret of policy Ψ through time t is

$$\text{Regret}(\Psi, P, t) = \mathbb{E}\left[\sum_{\tau=1}^{t}(\pi^* - \pi_{k_\tau} \mid \Psi, P, H_{\tau-1})\right] \tag{1}$$

where P is the set of prices being considered, π^* is the ex-post maximum expected profit in a given round, and π_{k_τ} is the profit realized when price p_k is played in time period τ. This metric[12] is used in the discussion of theoretical properties in Appendix EC.4.[13]

An alternative objective is to maximize the expected total reward (Gittins 1974, Cohen and Treetanthiploet 2020).[14] Formally, the goal is to pick a decision rule, Ψ, that selects a sequence of prices from the consideration set, P, that maximizes the total expected profit:

$$\mathbb{E}\left[\sum_{\tau=1}^{t}\pi_{k_t} \mid P\right] \tag{2}$$

We use this metric to discuss our empirical simulation results, as it is more intuitive in the context of the pricing problem (a firm maximizing profits through experimentation with an unknown demand curve). Additionally, if the true rewards distribution is unknown (e.g., in a field experiment), total rewards can still be compared, whereas regret lacks a straightforward alternative formulation. Another important criterion for businesses — especially those with few products unlikely to run many price experiments — is the variance of the expected total reward across simulations, with lower variance being preferable.

4.3. Baseline Policies — Deterministic and Stochastic Algorithms

Finally, we consider baseline policies, which serve as building blocks for our algorithm. The simplest approach is a fully randomized experiment (A/B testing), where a random arm is selected, ignoring the history of arms played and their outcomes. Another class includes myopic policies, such as greedy-based algorithms (e.g., ϵ-greedy) and softmax (Dann et al. 2022). In this paper, we build on two popular policies, UCB and TS, which form a fundamental component of many bandit algorithms.

[12] Formulating the bandit problem as a statistical problem (regret) rather than an optimization problem (maximizing cumulative reward) lends itself better to theoretical guarantees (Cohen and Treetanthiploet 2020).

[13] Theoretical guarantees often state that an algorithm has the lowest possible bound for expected regret; however, this is subtly different from empirical performance, which may be higher for algorithms without such theoretical properties. For example, it is proven that under certain conditions, UCB has the lowest possible bound for expected regret (Auer et al. 2002). However, empirically, under the same conditions, it is often outperformed by greedy algorithms with respect to maximizing rewards (Bayati et al. 2020).

[14] Among a set of algorithms, the one with the lowest cumulative regret is the same as the one with the highest cumulative rewards.

UCB: The Upper Confidence Bound (UCB) algorithm is a deterministic, nonparametric approach popularized for its proven asymptotic performance, achieving the lowest possible maximum regret (Lai and Robbins 1985, Agrawal 1995, Auer et al. 2002). The UCB policy scores each arm by summing an exploitation term and an exploration term, then selecting the arm with the highest score. The exploitation term is the sample mean of past rewards at a given arm, which provides information about past payoffs. The exploration term, meanwhile, increases with the uncertainty of the sample mean for an arm; specifically, it decreases as an arm is chosen more frequently and as the empirical variance of rewards at that arm decreases. Thus, the UCB policy balances exploitation and exploration.[15] To adapt UCB to pricing, we follow Misra et al. (2019) by scaling the exploration term by price (as shown in eq. (3)). This adjustment accounts for the known variation in the range of possible rewards at each arm, which is not generally assumed.

$$\begin{aligned} p_k^{\text{UCB}} &= \arg\max_{p_k \in P} \left(\bar{\pi}_{kt} + p_k \sqrt{\frac{\log(t)}{n_{kt}} \min\left(\frac{1}{4}, V_{kt}\right)} \right) \\ V_{kt} &= \left(\frac{1}{n_{kt}} \sum_{\tau=1}^{n_{kt}} \pi_{k\tau}^2 \right) - \bar{\pi}_{kt}^2 + \sqrt{\frac{2\log t}{n_{kt}}} \end{aligned} \tag{3}$$

TS: Thompson Sampling (TS) is a randomized Bayesian parametric approach. For each arm, a reward distribution is specified a priori and updated based on the history of past trials (Thompson 1933). In each round, an arm is chosen according to the probability that it is optimal, given the history of past trials. Specifically,

$$\text{Prob}(p_k \mid H_{t-1}) = \text{Prob}(E[\pi_{k,t} \mid p_k] > E[\pi_{k,t} \mid p_{k'}], \forall p_{k'} \neq p_k \mid H_{t-1}). \tag{4}$$

The simplest implementation is to sample from each distribution in each round and select the arm with the highest sampled payoff. In our setting, where purchase decisions are binary, the TS approach uses a scaled beta distribution, with parameters representing the number of successes and failures (Chapelle and Li 2011, Agrawal and Goyal 2012). Specifically, at time $t+1$ for each arm k, a sample is drawn from $\text{Beta}(s_{kt}+1, n_{kt}-s_{kt}+1)$ and then scaled by the price, p_{kt}. The arm with the highest value is chosen.

[15] If the exploration term were zero, this would be equivalent to a fully greedy algorithm.

5. Informational Externalities

In this section, we incorporate the two informational externalities into the baseline policies. Our objective is to create a general method that combines any decision rule (such as UCB, TS, or others) with the two relevant informational externalities. The first informational externality — continuity — is implemented using Gaussian process bandits developed by Srinivas et al. (2009). The main contribution of this paper, however, is the incorporation of the second externality — monotonicity — which also builds on the Gaussian process framework. An overview of how these externalities are incorporated into the baseline policies is shown in Figure 2.

Figure 2 **Overview of Incorporation of Informational Externalities**

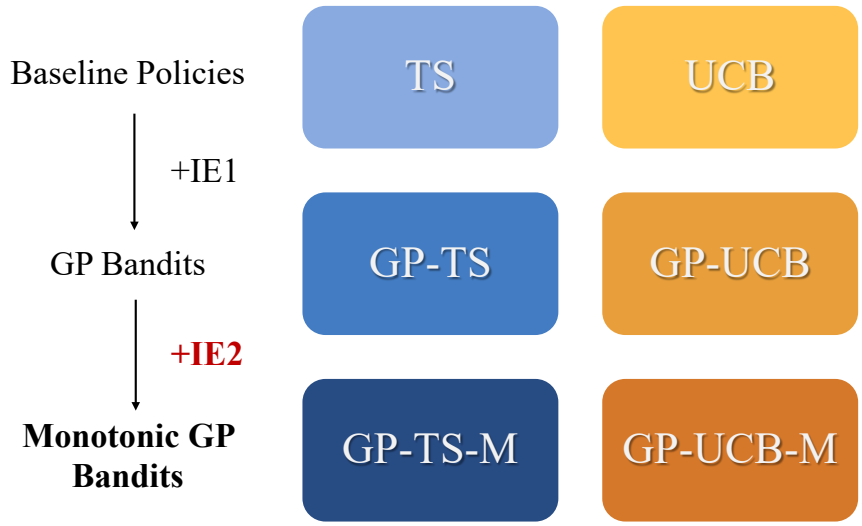

5.1. First Informational Externality: From Points to Functions

The first informational externality recognizes the local dependence of functions through continuity. Specifically, in the pricing application, we know that demands at two prices tend to be closer when the prices are closer together. To inform demand at arm j (price p_j), the demands at p_{j-1} and p_{j+1} are most informative. For example, knowing the demand at price $p = 0.5$ can be informative about the demand at $p = 0.6$. More generally, it is possible to learn about the demand $D(p)$ at price p from observed demands at nearby price points, such as $D(p+\epsilon)$ for small ϵ. The information spillover is bidirectional, with points further away being less important and weighted less due to the structure of the covariance matrix.

The logic of sharing information between arms means that using functions to model demand across the range of prices, rather than focusing on demand at specific arms (price

points), may lead to increased performance. A straightforward parametric approach would involve specifying functional forms (e.g., splines) to flexibly model the true demand curve, using observations only at the arms (prices). However, there is a risk that any parametric approximation chosen by the researcher may be insufficient to capture the true shape of the demand curve.

We take a more flexible nonparametric approach by modeling the space of demand functions as a Gaussian process (GP). A Gaussian process is a stochastic process (a collection of random variables) such that every finite subset has a multivariate Gaussian distribution; a simple example of fitting a GP to data can be found in Appendix EC.1. GPs can be thought of as a *probability distribution over possible functions*, allowing any function to be probabilistically drawn from the function space on the chosen support — unlike most commonly used methods in economics and marketing. Thus, any arbitrary demand curve can be modeled, and the GP learns the shape from the data. Following Srinivas et al. (2009), GPs can be incorporated into the bandit framework using both UCB and TS (Chowdhury and Gopalan 2017).

Advantages of GPs relative to other methods: GPs offer several desirable features for the present class of problems. First, GPs provide a parsimonious and nonparametric approach to incorporating both informational externalities in a transparent, principled, and provable manner.[16] Second, GPs have closed-form solutions that allow hyperparameters to be tuned quickly with maximum likelihood estimation. Intuitively, GPs work well with bandits because the exploration-exploitation trade-off relies on understanding the distribution of rewards, not just the mean reward at each arm.[17] A GP provides a probability distribution over functions, offering a principled way to manage the exploration-exploitation trade-off.

Finally, we note that other nonparametric methods, including many machine learning methods, may provide higher-accuracy estimates for the mean. However, because they are less capable of quantifying the certainty of their predictions, they are ill-suited for bandit algorithms, where managing the exploration-exploitation trade-off is crucial. In contrast, GPs can quantify uncertainty, allowing it to be incorporated into the decision-making

[16] An alternative approach would be to use a parametric model like *GLM-UCB* (Filippi et al. 2010) and restrict the coefficients to obtain weakly decreasing demand functions. Since we model demand based on a single variable, price, a nonparametric method is more flexible and less susceptible to model misspecification.

[17] This is also incorporated in the UCB algorithm, which models both a term for the sample mean of each arm and an exploration bonus dependent on the bounds surrounding those sample means.

process in a principled way. This is why a method like GPs is needed, as it estimates the entire distribution of functions when creating a smoothed alternative to the raw data. Indeed, one can consider using only the means of the posterior GP rather than the entire posterior.[18] This was tested in Srinivas et al. (2009), who found it was "too greedy too soon and tends to get stuck in shallow local optima" (p. 4), leading the algorithm to under-explore and produce inaccurate results.

5.1.1. Gaussian Processes The key building block of our approach, which underpins the modeling of both informational externalities, is the Gaussian process. In this section, we outline our implementation of modeling GPs in the pricing setting. As in Ringbeck and Huchzermeier (2019), we model the GP at the demand-level and then scale by price, allowing the bandit to make decisions at the reward-level.

Table 2 Summary of GP Notation

Description	Notation in Pricing Setting
Training data	$\mathcal{D}_t = \{P_t, y_t\}$
Noise hyperparameter	σ_y^2
RBF kernel	$k^{\text{RBF}}(p_i, p_j) = \sigma_f^2 e^{\frac{-(p_i - p_j)^2}{2l^2}}$
RBF hyperparameters	$\{\sigma_f, l\}$
Covariance function (kernel) evaluated at two points	$k(p_i, p_j)$
Covariance matrix between price vectors	$K(P, P)$

Training Data: The goal of estimating a GP is to learn the space of demand functions at test points, P,[19] given the purchase decision history obtained at time t from the MAB experiment. The training data is defined as $\mathcal{D}_t = \{P_t, y_t\}$, where $P_t = \{p_k : k \in K_t\}$ and $y_t = \{y_{kt} : k \in K_t\}$. Here, $K_t \subseteq K$ is the subset of actions tested by time t, and $y_{kt} = \frac{s_{kt}}{n_{kt}}$ represents the observed purchase rate for price p_k at time t. The purchase rates, y_{kt}, provide a noisy signal of the true value of the demand function $D(p)$ at p_k; specifically, we assume $y_{kt} = D(p_k) + \epsilon$, where $\epsilon \sim \mathcal{N}(0, \sigma_{y_k}^2)$. The vector $\sigma_y^2 = (\sigma_{y_1}^2, \ldots, \sigma_{y_K}^2)$ is referred to as the noise hyperparameter. Importantly, the cardinality of the training data depends on the number of prices in the test set, $|P| = K$, rather than increasing with t, the number of purchase decisions observed. The equivalence of these two approaches is discussed in Appendix EC.2.

[18] This approach can be thought of as a greedy-based GP algorithm.

[19] In our setup, we use only the prices from the test set, though it is possible to estimate for any arbitrary price.

Kernel: A Gaussian process flexibly models dependencies across input points using a kernel, implemented through a covariance function. A kernel $k(\cdot,\cdot)$ takes two points (in our setting, prices p_i and p_j) from the input space and returns a scalar representing the covariance between the outputs at those points. From this, a covariance matrix $K(\cdot,\cdot)$ can be constructed for a set of inputs.

A commonly used and robust kernel for GPs is the radial basis function (RBF) kernel, also known as the Gaussian kernel or the squared exponential kernel (Duvenaud 2014).

$$k^{\text{RBF}}(p_i,p_j)=\sigma_f^2 e^{-\frac{(p_i-p_j)^2}{2l^2}} \tag{5}$$

The RBF kernel has a set of desirable properties suited to our setting. It is differentiable and can provably approximate any arbitrary continuous target function uniformly on any compact subset of the input space (Micchelli et al. 2006).

Shape Hyperparameters: The RBF kernel has two shape hyperparameters, σ_f and l. The first hyperparameter, σ_f, is a scale factor that controls the amplitude of the function (i.e., the average distance of the function from its mean). The second hyperparameter, l, determines the smoothness[20] of the function, describing how the correlation between two points decreases as the distance between them increases (Shahriari et al. 2015).

A crucial practical step in estimating the GP is tuning the hyperparameters. To minimize human (researcher) judgment, it is ideal to have an efficient, accurate, and automatic method for selecting hyperparameters. We use standard non-Bayesian methods for tuning the hyperparameters.[21] This approach involves choosing values of the hyperparameters that maximize the likelihood of the data given the model. Mathematically, this is equivalent to minimizing the negative log marginal likelihood (equation 2.30 in Williams and Rasmussen (2006)):

$$\log \text{prob}(y_t|P_t)=-\frac{1}{2}y_t^T(K(P_t,P_t)+\sigma_y^2 I)^{-1}y_t-\frac{1}{2}\log|K(P_t,P_t)+\sigma_y^2 I|-\frac{t}{2}\log(2\pi) \tag{6}$$

Noise Hyperparameter: While the noise hyperparameter can be estimated along with the shape hyperparameters, we choose to specify it directly due to the difficulty in disentangling shape and noise hyperparameters (Murray 2008).[22] We use the fact that purchase

[20] Intuitively, this can be thought of as the length of the "wiggles."

[21] Bayesian tuning methods are often too slow and not suitable for real-time bandit settings.

[22] For example, consider two close input points (x-axis) that have very different outputs (y-axis). One possible explanation is that the data is accurate, and the GP requires shape parameters that permit sufficiently high variation to capture large output differences from nearby inputs. Alternatively, the true outputs may be close together, but the data is very noisy; in this case, the previous shape parameters would be overfitting.

decisions are binary in our model to characterize the upper bound of the variance at any price. As prices are set within the interval $[0, 1]$, the variance for a Bernoulli random variable is $p(1-p)$, which implies that the maximum variance in purchase probability is 0.25, occurring when the true purchase probability is $p = 0.5$. Thus, a conservative approach, without estimating the noise hyperparameter, would be to set the noise variance to 0.25 for all prices.[23] While this may be overly conservative for some prices, setting noise hyperparameters too low could limit exploration and lead to poor results by causing the algorithm to get stuck in errant equilibria. A discussion of alternative methods, where noise takes on different values for different prices (i.e., heteroscedastic noise), is provided in Appendix EC.8.

Posterior Prediction: Estimating the posterior GP from the training data is done using standard GP regression. The equations and a simple illustrative example are provided in Appendix EC.1.

5.1.2. GP-UCB and GP-TS Gaussian processes can be combined with bandits, such as UCB (Srinivas et al. 2009) and TS (Chowdhury and Gopalan 2017), to create *GP-UCB* and *GP-TS*, respectively. The general idea is that instead of using the raw data directly, a posterior GP is estimated before applying a UCB scoring rule or Thompson sampling. Our implementations of these algorithms are standard and follow the prior literature. The only adjustment needed to apply these algorithms in the pricing setting is to scale by price, an approach also used in Ringbeck and Huchzermeier (2019). This adjustment is necessary because bandits make decisions at the reward (profit) level, while the GP learns at the demand level.

To initialize the algorithm, we select the first price randomly.[24] Once one data point is available, the training data $\mathcal{D}_t = \{P_t, y_t\}$ can be used to choose the hyperparameters using equation (6). Additionally, the posterior mean $\mu(D^*)$ and covariance matrix $\mathrm{Cov}(D^*)$ can be calculated using equations (EC.5) and (EC.6).[25]

[23] As we use purchase rates rather than purchase decisions as the training data, we also need to divide by n_{kt} at each price. See Appendix EC.2 for details.

[24] Another possible initialization method is to set arbitrary hyperparameters and model the GP without data. Both methods are practical, with only minor differences in overall performance (under 1% in all our simulations), and neither method consistently outperforms the other.

[25] D^* is a random variable denoting the Gaussian process posterior prediction.

With the GP estimated, UCB and TS can be applied. For GP-UCB, at each price $p_k \in P$, the posterior demand mean $\mu_t(p_k)$ and posterior variance $\sigma_t^2(p_k)$ are used to determine the price at iteration $t+1$ according to the following decision rule:

$$p_k^{\text{GP-UCB}} = \arg\max_{p_k \in P} \left(p_k \left(\mu_t(p_k) + \beta_{t+1}^{1/2} \sigma_t(p_k) \right) \right) \tag{7}$$

where $\beta_t = \frac{2}{5} \log(|P| t^2 \pi^2 / (6\delta))$, with δ set to 0.1.[26] Note that we have scaled by p_k as the algorithm is optimizing for reward rather than demand (the level at which the GP was estimated).

On the other hand, in GP-TS, rather than sampling at each arm as in traditional TS, a demand draw for every test price, $d_t(p_k)$, can be obtained by sampling from the posterior GP. Specifically, $d_t(p_k)$ is a sample from the posterior normal distribution with the given mean and covariance matrix, $D^* \sim N(\mu(D^*), \text{Cov}(D^*))$. Then, using Thompson sampling, the selected price will be

$$p_k^{\text{GP-TS}} = \arg\max_{p_k \in P} (p_k d_t(p_k)) \tag{8}$$

5.2. Second Informational Externality: Monotonicity

We now focus on the main contribution of this paper: incorporating the second informational externality into Gaussian process bandits. The monotonicity property has a global influence, as demand at price p_j constrains all demands at higher prices, since $D(p_k) \leq D(p_j)$ when $p_k \geq p_j$. This impact is also asymmetric: specifically, demand at a higher price p_k is upper-bounded by demand at a lower price p_j, while demand at a lower price is lower-bounded by demand at a higher price.

We aim to remain fairly agnostic between GP-UCB and GP-TS, as past literature (Chowdhury and Gopalan 2017) shows that neither completely dominates the other. This means our method must be general enough to integrate with both GP-UCB and GP-TS. We will refer to the monotonicity versions of GP-UCB and GP-TS as *GP-UCB-M* and *GP-TS-M*, respectively. The goal is to determine whether and under what conditions incorporating monotonicity improves performance for either variant.

When using GP-TS or GP-UCB, the baseline GP allows for any demand function and does not impose any restrictions on the shape. To be consistent with the assumption that

[26] This is the value that Srinivas et al. (2009) found empirically to work well. Other values of β may perform better in different simulations, though determining β without past data is generally challenging (Hoffman et al. 2011).

demand weakly decreases with price, our goal is to obtain only weakly decreasing functions. For GP-TS-M, we require a way to randomly draw a monotonic function from the set of monotonic functions in the posterior GP. For GP-UCB-M, we require an estimate of the mean and variance from the subset of monotonic demand curves from the posterior; alternatively, this can be approximated by averaging over multiple monotonic draws.

To obtain a random monotonic draw, a simple approach is to use rejection sampling by repeatedly sampling from the GP until a weakly decreasing draw is obtained. While this approach can work, there is no guarantee that a weakly decreasing draw will be found quickly. This issue is further exacerbated when there are few observations or many test prices; when faced with many arms and (noisy) non-monotonic sample means, the probability of finding a monotonic draw can become vanishingly small.

To ensure that a weakly decreasing draw can be obtained from a GP expediently in all cases, we develop a method from first principles. Although sampling a monotonic function from a GP is intractable, obtaining a draw from a GP where all values are negative is a tractable sampling problem (equivalent to sampling from a truncated normal). Specifically, since a decreasing monotonic function can be characterized by having negative first derivatives at all points, if a link exists between the GP and its derivatives, we can transform the monotonic sampling problem into a tractable one. We establish this link by leveraging the property that the derivative of a GP is also a GP (and that the RBF kernel we use is infinitely differentiable), allowing us to estimate the derivative of the GP from our data. We then use the basis functions proposed by Maatouk and Bay (2017) to recover the demand function estimate from a draw of negative derivatives sampled from the derivative of the GP.

Another advantage of this principled approach is that the function is guaranteed to be monotonic not only at the discrete price levels forming the support but also at any intermediate price where no experimentation is performed. This ensures consistency in the function's behavior across the entire price range. The only assumption required is that the demand function is differentiable with a continuous derivative.

5.2.1. Basis Functions To estimate the demand function, we use a collection of functions h_j known as the interpolation basis. These basis functions are defined a priori and remain the same regardless of the input data. They provide a method for estimating a function at all points by linearly interpolating between known function values at knots spaced

over the support. Following the notation of Maatouk and Bay (2017), let $u_j \in [0,1]$, for $j = 0, 1, \ldots, N$, denote equally spaced knots on $[0,1]$ with spacing $\delta_N = 1/N$ and $u_j = j/N$. The interpolation basis is defined as

$$h_j(p) = h\left(\frac{p - u_j}{\delta_N}\right) \text{ where } h(p) = (1 - |p|)\mathbb{1}(p \in [-1,1]). \tag{9}$$

Then, for any continuous function $D : [0,1] \to \mathbb{R}$, the function

$$D_N(\cdot) \approx \sum_{j=0}^{N} D(u_j) h_j(\cdot) \tag{10}$$

approximates D by linearly interpolating between function values at the knots u_j. A key property of the interpolation basis is that, as the gap between the evenly spaced knots becomes infinitesimally small, the distance between the estimate and the true function converges to 0.

Our goal, however, is to simplify the sampling problem by approximating the demand function in terms of its derivatives at the knot points. Equation 10 can be transformed to express the demand function in terms of its intercept, derivatives, and the original basis functions h_j, as shown in Proposition 1 (a derivation is provided in Appendix EC.3.2). Appendix EC.3.1 provides a visual demonstration of the basis functions h_j and their integrals $\int_0^p h_j(x)\,dx$.

PROPOSITION 1. *Assuming a demand function $D : [0,1] \to \mathbb{R}$ is differentiable with a continuous derivative (i.e., $D \in C^1([0,1])$), it can be estimated by its intercept and derivatives using the following equation:*

$$D(p) \approx D(0) + \sum_{j=0}^{N} D'(u_j) \int_0^p h_j(x)dx \tag{11}$$

While this approach applies to all class C^1 functions on the support, we additionally assume that the unknown demand function D is weakly decreasing, meaning that it belongs to a subset $\mathcal{M}$ defined as follows:

$$\mathcal{M} \coloneqq \{D \in C^1([0,1]) : D'(p) \leq 0, p \in (0,1)\} \tag{12}$$

In other words, D belongs to the subset of functions where the derivative is never positive at any value of p.

5.2.2. GP-UCB-M and GP-TS-M To summarize, the main differences between the monotonic and non-monotonic versions of GP bandits are as follows. When incorporating monotonicity, instead of estimating a GP of the means at the test prices, we estimate a GP of the derivatives at the knots, concatenated with the mean at the intercept. Crucially, the intercept and derivatives must be estimated together, which is possible due to the property of a GP that the joint distribution of values and their derivatives is also a GP (Appendix EC.3.3 provides details on calculating the derivative of a GP). Once the posterior GP is estimated, off-the-shelf sampling can be used to acquire a draw where every derivative is non-negative (we use the *TruncatedNormal* package in R (Botev and Belzile 2021)). We denote $\mathcal{M}$ as the subset of monotonically decreasing functions from the posterior GP. Then, equation (11) provides a formula to recover the demand sample d at the desired test prices using only the draw and basis functions h. From this point, the decision rules for GP-UCB or GP-TS can be applied as usual. Formally, the methods are outlined in Algorithms 1 and 2.

Algorithm 1: GP-TS-M

Set test prices P, kernel k, noise hyperparameter σ_y^2, and knots $\mathcal{U}$
Compute the integrals of the basis functions at $\mathcal{U}$ using equation (9)
Define test points as $\mathcal{U}_0 = \{0\} \cup \mathcal{U}$ (concatenate the intercept)
For $t = 1$ pick price randomly, and observe purchase decision
Initialize training input P_t and training output y_t
for $t = 2, 3, ...$ **do**
    Compute shape hyperparameters σ_f and l using equation (6)
    Compute covariance matrix (equation (EC.3)) using P_t and $\mathcal{U}_0$ with equations (EC.11), (EC.12), (EC.13)
    Estimate posterior GP using equations (EC.5) and (EC.6)
    Sample randomly from $\mathcal{M}$ at test points $\mathcal{U}_0$
    Estimate the demand draw d_t at test prices P using equation (11)
    Play price $p_k = \arg\max_{p_k \in P} (p_k d_t(p_k))$
    Observe purchase decision
    Update P_t and y_t
end

Algorithm 2: GP-UCB-M

Set test prices P, kernel k, noise hyperparameter σ_y^2, and knots $\mathcal{U}$
Compute the integrals of the basis functions at $\mathcal{U}$ using equation (9)
Define test points as $\mathcal{U}_0 = \{0\} \cup \mathcal{U}$ (concatenate the intercept)
For $t = 1$ pick price randomly, and observe purchase decision
Initialize training input P_t and training output y_t
for $t = 2, 3, ...$ **do**
    Compute shape hyperparameters σ_f and l using equation (6)
    Compute covariance matrix (equation (EC.3)) using P_t and $\mathcal{U}_0$ with equations (EC.11), (EC.12), (EC.13)
    Estimate posterior GP using equations (EC.5) and (EC.6)
    Obtain N samples from $\mathcal{M}$ at test points $\mathcal{U}_0$
    Estimate the demand draw $d_{t,n}$ at test prices P using equation (11) for each of the N samples
    Estimate $\mu_t(p_k)$ and $\sigma_t(p_k)$ from the collection of demand draws
    Play price $p_k = \arg\max_{p_k \in P} \left(p_k \left(\mu_t(p_k) + \beta_{t+1}^{1/2} \sigma_t(p_k) \right) \right)$
    Observe purchase decision
    Update P_t and y_t
end

5.2.3. Theoretical Properties Finally, we discuss some theoretical properties of our algorithms. Our main theoretical result shows a regret with a main term that scales like $O\left(\mathbb{E}\left[\sqrt{\gamma_T \sum_{t=1}^{T} p_t^2}\right]\right)$ where γ_T is a problem dependent quantity reflecting the underlying effective dimension of the kernel, and p_t is the price played at time t. Our analysis follows the standard approach of Thompson sampling for Gaussian processes; we refer the reader to Srinivas et al. (2009) for more details on the interpretation of γ_T. We note that, in the case of the RBF kernel, γ_T is $\log(T)$ and so has a negligible contribution to the regret. As we discuss in Appendix EC.4, the regret also consists of a smaller term E_T, which we show empirically is bounded by a sublinear term.

The most interesting aspect of the regret is the improved "path-dependent" analysis, which reflects the actual prices played and demonstrates the advantage of exploiting the monotonic structure (Zhao et al. 2023). At worst, if we naively upper bound p_t by 1, this yields a regret of $O(\sqrt{\gamma_T T})$. However, this expression does not capture the true behavior of our proposed method. Intuitively, since we are achieving sub-linear regret, we expect that, as time progresses, the price p_t converges to p_* as $t \to \infty$. Thus, for large T, our regret is closer to $p_* \sqrt{T} \leq p\sqrt{T}$.

Furthermore, as we discuss in Section 3.1, by multiplying the demand by p, we are effectively create larger confidence intervals (and thus greater uncertainty) for profit at higher prices, while lower prices yield smaller confidence intervals and less uncertainty on the profit curve. Consequently, p_t may be very large in the earlier rounds as the algorithm strives to reduce uncertainty on the profit at higher prices — regardless of whether we use UCB or Thompson sampling. By enforcing monotonicity, this effect is still present but mitigated, as $D(p)$ is necessarily smaller for larger values of p, even if we have not fully learned the function at those values. As a result, the p_t we ultimately play should be smaller than it would be without monotonicity enforced.

6. Analysis and Results

We now explain the implementation of the algorithms, specifically detailing key components such as consumer valuations, the number of arms, and the sequence of events in the multi-armed bandit.

Sequence of Events: We evaluate our proposed algorithm and benchmarks using simulations based on a standard setup for assessing bandit algorithms in pricing (Misra et al. 2019). Each simulation has the following structure. First, at each time period, a potential buyer (consumer) arrives from a large pool of consumers by being drawn from an unknown WTP distribution. They are shown a price chosen by the algorithm (which has no specific knowledge about this consumer), and they decide to purchase one unit if and only if their valuation for the product is greater than the price shown. The outcome (purchase or no purchase) is observed by the algorithm, which then updates its history of observations. We allow for the algorithm to update its price every 10 consumers.[27]

Varying the Number of Arms: When choosing the number of arms (prices) to test, the decision maker must balance two competing considerations: the granularity of the price set and the complexity of the learning problem. A smaller set of test prices may result in the best price within the set being far from the true optimal price. Conversely, testing a larger set of prices increases the complexity of learning, which can slow down convergence and potentially lead to higher cumulative losses. We evaluate performance across different price sets, normalized from 0 to 1, using intervals corresponding to 100 arms, 10 arms, and 5 arms.

[27] While prices could be updated every period (i.e., for each consumer), this may be impractical in real-world settings. To better reflect industry practices, we change prices every 10 consumers, as in Misra et al. (2019).

Valuation (WTP) Distributions: Right-skewed, Left-skewed, and Symmetric: To evaluate the performance of various MAB policies, it is crucial to consider different shapes of consumer valuation (WTP) distributions. Following Misra et al. (2019), we analyze three types of distributions using specific parameterizations of the Beta distribution: Beta(2,9) for a right-skewed distribution, Beta(9,2) for a left-skewed distribution, and Beta(2,2) for a symmetric distribution. A graphical depiction of the willingness to pay, the demand curve, and the profit curve for each simulation setting is provided in Figure 3. A monopolist with perfect knowledge of the demand curve would set prices to maximize profit. The true optimal prices are 0.15 for Beta(2,9), 0.42 for Beta(2,2), and 0.68 for Beta(9,2).

Figure 3 WTP Distributions and Demand and Profit Functions

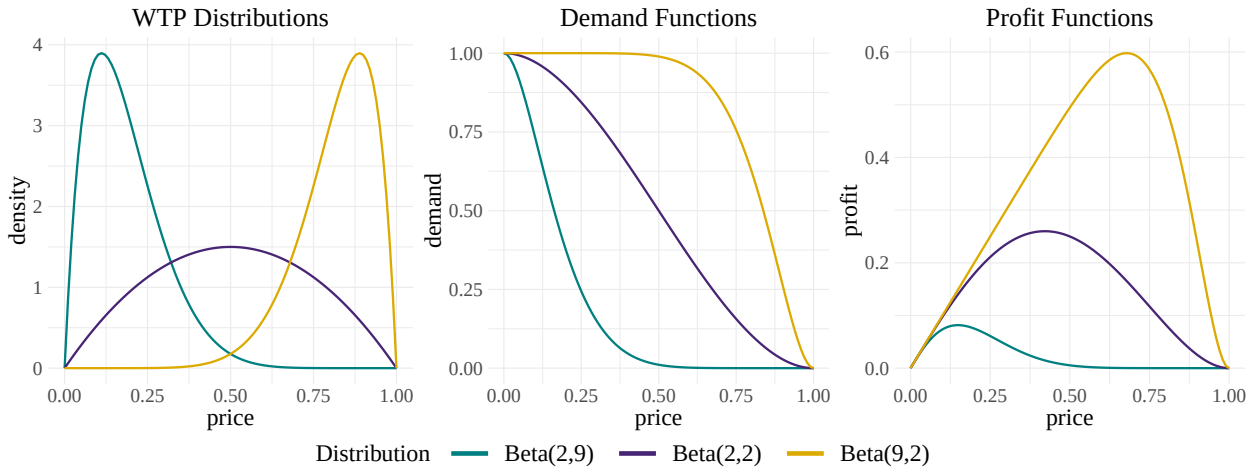

Initializing the Algorithm: The algorithms are initialized with either a prior or limited experimentation. For UCB, we assume a prior that encourages exploration by treating every untested price as if it has been tested once and resulted in a purchase.[28] In contrast, TS- and GP-variants can use uninformed priors, enabling price selection even without prior data. To make the comparison more consistent,[29] we have GP-variants select the first price randomly, after which the price can be chosen using the data-estimated GP.

[28] An alternative approach is to test each price before applying the UCB policy; however, our initialization priors allow for the possibility of not testing every price, which can improve algorithmic performance.

[29] When faced with an uninformed prior, there are slight differences in the distribution of the first price chosen by the monotonic and non-monotonic algorithms. This can lead to minute differences in performance (under 1% and usually around 0%) depending on the underlying WTP distribution attributable solely to the first price decision, which we mitigate by choosing the first price randomly.

6.1. Results

Our results present several variants within two main classes of algorithms (TS and UCB). Figure 4 illustrates the cumulative performance of each algorithm over time (or number of consumers), while Table 3 provides the exact values from this figure at 500 and 2500 consumers. Table 4 shows the uplift, or gains, from incorporating the two informational externalities relative to the baseline algorithms. Finally, Figure 5 presents a histogram of prices played, offering insight into the behavior of the different algorithms.

6.1.1. Main Results: Cumulative Performance The performances of the algorithms are shown in Figure 4, which reports the cumulative percentage of optimal rewards relative to the case when the optimal arm (price) is played.[30] In each subfigure, the horizontal black dotted line represents the maximum obtainable rewards given the price set (i.e., the ratio of the reward obtained from playing the best price within the price set to the true optimal reward). The value of this line increases as the price set enlarges, approaching the true optimal of 100%. Visually, algorithms with no informational externalities are represented with dots, those with the first informational externality (i.e., the GP) are represented with dashes, and those with both informational externalities are represented with solid lines. UCB-variants are shown in warm (orange-based) colors, while TS-variants are in cool (blue-based) colors.

In general, the results show that incorporating informational externalities improves algorithmic performance, though the effects vary across distributions and the number of arms. We explore this in more detail, starting with 5 arms [Figure 4a)]. For the right-skewed Beta(2,9) distribution, there is a significant separation in algorithmic performance even after 2500 consumers, despite all algorithms eventually converging to the optimal price with sufficient learning. Incorporating the first informational externality – a Gaussian process – results in minimal improvement for UCB and a slight decrease in performance for TS. However, incorporating the second informational externality – monotonicity – leads to substantial performance gains for both GP-UCB and GP-TS. Finally, the Nonparametric TS (N-TS) algorithm performs well relative to most other algorithms but is outperformed by GP-TS-M.

[30] There are two sources of variation between simulations: one from the algorithm itself and another from the exact WTP draws from the true distribution. Using expected rewards from playing a price reduces the variation caused by WTP draws, allowing for a cleaner comparison of algorithmic performance. Misra et al. (2019) also use expected rewards in their analysis.

Figure 4 Cumulative Percent of Optimal Rewards (Profits)

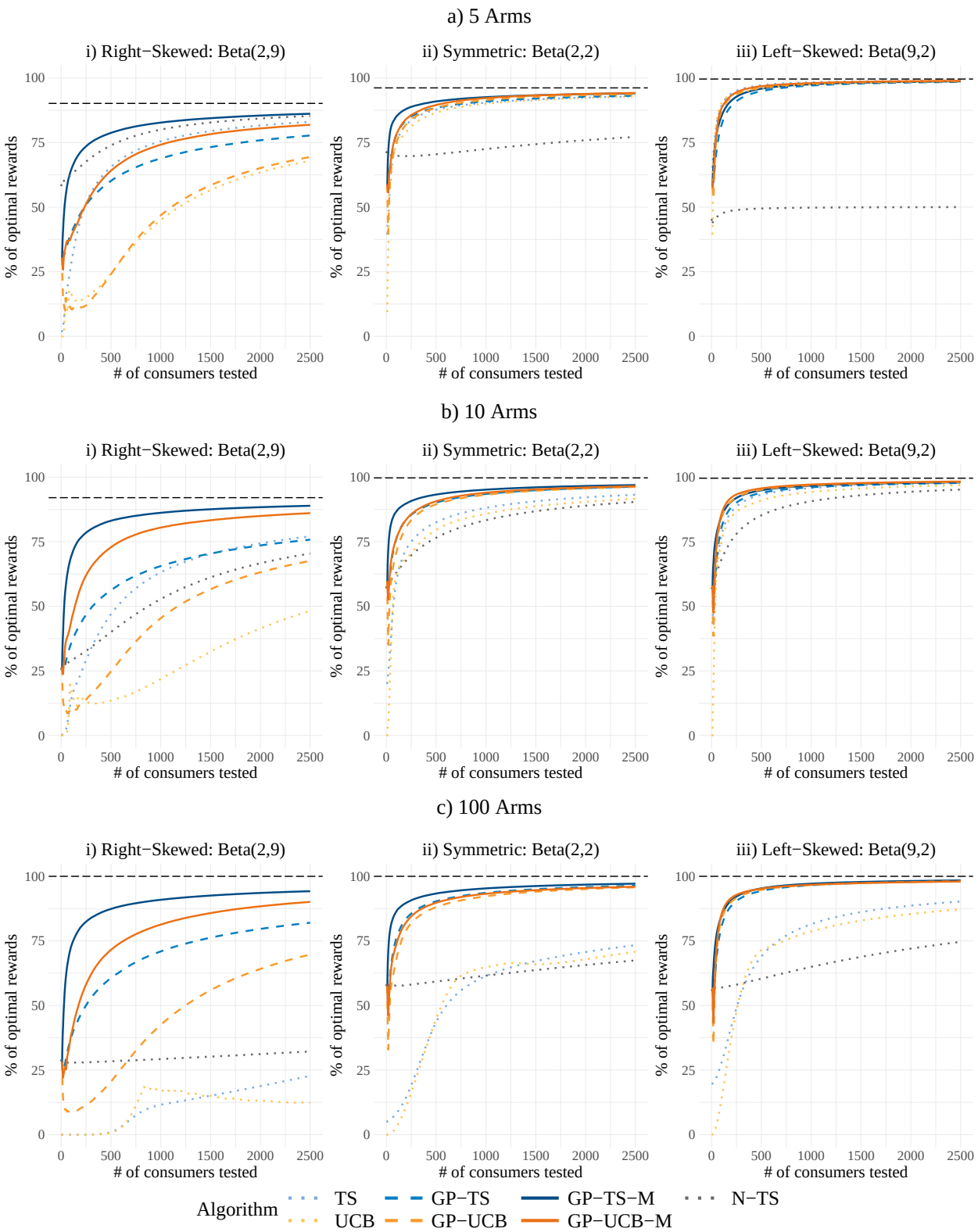

Notes. The lines represent the means of the cumulative expected percentage of optimal rewards across 1000 simulations. The black horizontal line represents the maximum obtainable reward given the price set, while 100% represents the true optimal reward given the underlying distribution.

Table 3 Cumulative Percent of Optimal Rewards (Profits)

	After 500 Consumers							
	% of Price Set Maximum Reward				% of True Optimal Reward			
Algorithm	**B(2,9)**	**B(2,2)**	**B(9,2)**	**Mean**	**B(2,9)**	**B(2,2)**	**B(9,2)**	**Mean**
				5 Arms				
TS	72.7	91.2	97.6	**87.2**	65.6	87.7	97.2	**83.5**
GP-TS	66.7	92.0	95.3	**84.7**	60.2	88.4	94.9	**81.2**
GP-TS-M	87.3	94.6	96.3	**92.7**	78.7	90.9	95.9	**88.5**
N-TS	82.0	73.3	49.7	**68.3**	73.9	70.5	49.5	**64.6**
UCB	27.0	90.0	96.5	**71.1**	24.3	86.5	96.1	**69.0**
GP-UCB	26.6	92.0	96.6	**71.8**	24.0	88.5	96.2	**69.6**
GP-UCB-M	71.1	93.1	97.2	**87.1**	64.1	89.5	96.8	**83.5**
				10 Arms				
TS	51.0	82.8	93.6	**75.8**	46.9	82.5	93.2	**74.2**
GP-TS	61.1	90.4	94.3	**81.9**	56.2	90.1	93.9	**80.1**
GP-TS-M	90.3	93.5	95.3	**93.0**	83.1	93.3	94.9	**90.4**
N-TS	43.5	76.8	85.6	**68.6**	40.0	76.5	85.2	**67.3**
UCB	14.6	79.8	91.4	**61.9**	13.5	79.6	91.0	**61.3**
GP-UCB	27.0	89.8	95.6	**70.8**	24.8	89.5	95.2	**69.8**
GP-UCB-M	79.1	90.9	96.1	**88.7**	72.9	90.7	95.7	**86.4**
				100 Arms				
TS	1.0	43.5	69.0	**37.8**	1.0	43.5	69.0	**37.8**
GP-TS	60.6	90.3	94.3	**81.8**	60.6	90.3	94.3	**81.8**
GP-TS-M	87.4	93.3	95.3	**92.0**	87.4	93.3	95.3	**92.0**
N-TS	28.4	59.3	60.4	**49.3**	28.4	59.3	60.4	**49.3**
UCB	0.7	44.8	71.4	**39.0**	0.7	44.8	71.4	**39.0**
GP-UCB	20.5	88.1	94.8	**67.8**	20.5	88.1	94.8	**67.8**
GP-UCB-M	71.5	89.8	95.2	**85.5**	71.5	89.8	95.2	**85.5**
	After 2500 Consumers							
	% of Price Set Maximum Reward				% of True Optimal Reward			
Algorithm	**B(2,9)**	**B(2,2)**	**B(9,2)**	**Mean**	**B(2,9)**	**B(2,2)**	**B(9,2)**	**Mean**
				5 Arms				
TS	92.1	96.6	99.4	**96.1**	83.0	92.9	99.0	**91.7**
GP-TS	86.2	96.9	98.9	**94.0**	77.7	93.2	98.5	**89.8**
GP-TS-M	95.6	97.8	99.1	**97.5**	86.1	94.1	98.7	**93.0**
N-TS	94.6	80.3	50.2	**75.0**	85.3	77.2	50.0	**70.8**
UCB	75.4	96.6	99.1	**90.4**	68.0	92.9	98.7	**86.5**
GP-UCB	77.0	97.5	99.2	**91.2**	69.4	93.8	98.8	**87.3**
GP-UCB-M	90.8	98.0	99.3	**96.0**	81.9	94.2	98.9	**91.7**
				10 Arms				
TS	83.7	93.5	98.1	**91.8**	77.1	93.2	97.7	**89.3**
GP-TS	82.3	96.6	98.2	**92.4**	75.8	96.3	97.7	**89.9**
GP-TS-M	96.6	97.2	98.4	**97.4**	88.9	96.9	98.0	**94.6**
N-TS	76.5	90.7	95.6	**87.6**	70.4	90.4	95.2	**85.3**
UCB	52.4	91.9	97.3	**80.5**	48.3	91.6	96.9	**78.9**
GP-UCB	73.4	96.5	98.6	**89.5**	67.6	96.2	98.2	**87.3**
GP-UCB-M	93.5	96.8	98.7	**96.3**	86.1	96.5	98.3	**93.6**
				100 Arms				
TS	22.8	73.3	90.2	**62.1**	22.8	73.3	90.2	**62.1**
GP-TS	82.0	96.3	98.2	**92.2**	82.0	96.3	98.2	**92.2**
GP-TS-M	94.2	97.1	98.4	**96.6**	94.2	97.1	98.4	**96.6**
N-TS	32.2	67.4	74.6	**58.1**	32.2	67.4	74.6	**58.1**
UCB	12.4	70.8	87.2	**56.8**	12.4	70.8	87.2	**56.8**
GP-UCB	69.7	95.7	98.1	**87.8**	69.7	95.7	98.1	**87.8**
GP-UCB-M	90.1	96.0	98.0	**94.7**	90.1	96.0	98.0	**94.7**

Next, we examine the symmetric and left-skewed distributions, Beta(2,2) and Beta(9,2), respectively. While the ordering of algorithms' performance is similar to the right-skewed Beta(2,9) case, the differences begin to shrink. This aligns with expectations outlined in Section 3, as the learning problem becomes easier when the optimal price is higher within the price set, allowing all algorithms to perform well. The one exception is N-TS, which

performs worse in these cases. Averaging across all three distributions, the best-performing algorithm is GP-TS-M, achieving 92.7% of the maximum reward obtainable given the price set (88.5% of the true optimal) after 500 consumers and 97.5% (93.0% of the true optimal) after 2500 consumers (see Table 3).

While GP-TS-M performs best across the three distributions, GP-UCB shows only a slight improvement over UCB, and GP-TS performs worse than TS. This outcome might seem counterintuitive, as providing the algorithm with more information could be expected to increase profits. However, the advantage of using a GP lies in its ability to learn from nearby arms, which is limited when there are only five widely spaced arms. Additionally, a drawback of using a GP is that it relies on a single noise hyperparameter, while the true underlying noise varies with price. If this drawback outweighs the benefit of shared learning, GP-TS can perform worse. We address this limitation by introducing heteroscedastic noise in Appendix EC.8.

As the number of arms increases from 5 to 10, the rank ordering of the algorithms remains similar, with a few notable differences. In the Beta(2,9) case, the first informational externality allows GP-TS to initially outperform TS, though TS narrowly surpasses it by 2500 consumers. In contrast, GP-UCB now significantly outperforms UCB. Similarly, in both the Beta(2,2) and Beta(9,2) cases, the performance gap between GP-TS (GP-UCB) and TS (UCB) widens. Accordingly, the variation in performance across algorithms increases, with the lower-performing algorithms falling further behind the best-performing ones. This growing difference occurs because of the first informational externality. Meanwhile, the second informational externality again provides a substantial gain in the Beta(2,9) case but only minor improvements in the Beta(2,2) and Beta(9,2) cases. GP-TS-M continues to lead in performance, while N-TS performs comparably to TS and UCB.

When the number of arms increases from 10 to 100, these patterns intensify. The gap between the best- and worst-performing algorithms widens further, driven primarily by the benefits of the first informational externality, which grows as the number of arms increase. Learning across 100 arms without leveraging nearby information requires significantly more data, making the advantages of shared learning through a Gaussian process increasingly pronounced. The second informational externality maintains similar effects regardless of the number of arms, reinforcing the substantial gain in the Beta(2,9) case while providing

only minor improvements in the Beta(2,2) and Beta(9,2) cases. GP-TS-M remains the best-performing algorithm, with N-TS still performing similarly to TS and UCB.

Having discussed the results for various price granularities (number of arms), a question remains: in practice, a priori, how should a firm choose the price set? The general trade-off is that learning the optimal is easier (more efficient) with fewer prices, but a higher optimum is possible when more prices are considered.

To illustrate, in the Beta(9,2) case with 5 arms and after 2500 consumers, GP-TS-M achieves 99.1% of the maximum reward possible given the chosen price set, which equates to 98.7% of the true optimal reward. Meanwhile, at the higher price granularity of 100 arms, GP-TS-M achieves 98.4% of both the maximum reward possible and the true optimal reward. In this case, the maximum reward possible with 5 arms happens to be close enough to the true optimal that the benefits of an easier learning problem outweigh the potential gains from being able to select a price closer to the true optimal. This is not always true. In the Beta(2,9) case, the maximum reward possible is just 90.2% of the true optimal. As a result, despite GP-TS-M obtaining 95.6% of the maximum reward possible with 5 arms, it achieves just 86.1% of the true optimal – much worse than 100 arms which achieves 94.2%.

Overall, averaged across the three distributions, the highest-performing algorithm relative to the true optimal is GP-TS-M with 100 arms. Thus, we suggest firms use many arms,[31] as this allows for higher potential gains that outweigh the losses from a more challenging learning problem, which are significantly mitigated by the incorporation of informational externalities. Additionally, GP-TS-M with 100 arms is also the best-performing algorithm after 500 consumers, making this advice applicable for experiments of any reasonable length.[32]

6.1.2. Uplifts: Performance Increase from Informational Externalities Next, we examine the uplifts (the percentage improvement in cumulative profits from including an informational externality) in Table 4. This analysis not only quantitatively assesses the value of the externalities but also clarifies how their impact interacts with different distributions and numbers of arms. Overall, we observe that while the uplift from the first

[31] Across the three distributions we tested, with 100 arms the maximum reward obtainable was at least 99.99% of the true optimal, suggesting that 100 arms may be sufficient. Further testing on a wider variety of WTP distributions is needed to be more conclusive.

[32] If the experiment becomes sufficiently short, there will eventually be a point where a smaller price set will perform better.

Table 4 Uplifts in Performance from Informational Externalities

		After 500 Consumers					
		TS			**UCB**		
		5 Arms	10 Arms	100 Arms	5 Arms	10 Arms	100 Arms
Uplift from 1st externality (GP compared to base algos)	**B(2,9)**	-8.0% (-8.6, -7.3)	20.6% (19.2, 22.1)	5940% (5840, 6040)	2.0% (0.0, 4.1)	92.1% (86.6, 97.6)	2720% (2650, 2790)
	B(2,2)	1.0% (0.6, 1.3)	9.4% (9.0, 9.8)	108% (107, 109)	2.4% (2.0, 2.7)	12.6% (12.1, 13.1)	96.6% (96.0, 97.2)
	B(9,2)	-2.4% (-2.5, -2.2)	0.8% (0.6, 1.0)	36.8% (36.6, 37.1)	0.1% (0.0, 0.3)	4.6% (4.5, 4.8)	32.7% (32.6, 32.8)
	Mean	**-2.8% (-3.1, -2.6)**	**8.2% (7.8, 8.5)**	**116% (115, 117)**	**0.9% (0.7, 1.2)**	**14.3% (13.9, 14.7)**	**73.9% (73.4, 74.4)**
Uplift from 2nd externality (GP-M compared to GP algos)	**B(2,9)**	31.5% (30.5, 32.5)	50.1% (48.4, 51.8)	45.5% (44.1, 47.0)	176% (170, 182)	237% (222, 252)	296% (281, 310)
	B(2,2)	2.9% (2.6, 3.2)	3.5% (3.2, 3.9)	3.4% (3.1, 3.8)	1.3% (1.0, 1.6)	1.4% (1.0, 1.8)	2.1% (1.6, 2.5)
	B(9,2)	1.0% (0.9, 1.2)	1.1% (1.0, 1.2)	1.1% (0.9, 1.2)	0.6% (0.5, 0.7)	0.5% (0.4, 0.6)	0.5% (0.4, 0.5)
	Mean	**9.6% (9.3, 9.8)**	**13.7% (13.3, 14.0)**	**12.6% (12.3, 12.9)**	**21.5% (21.1, 21.9)**	**25.6% (25.1, 26.0)**	**26.3% (25.9, 26.7)**
Uplift from both externalities (GP-M compared to base algos)	**B(2,9)**	20.4% (19.6, 21.3)	78.5% (76.9, 80.0)	8610% (8470, 8740)	174% (168, 179)	468% (457, 479)	975% (970, 980)
	B(2,2)	3.8% (3.5,4.1)	13.2% (12.7, 13.6)	115% (114,116)	3.6% (3.2, 3.9)	14.1% (13.6, 14.5)	100% (100, 101)
	B(9,2)	-1.4% (-1.5, -1.2)	1.9% (1.7, 2.1)	38.3% (38.0, 38.6)	0.8% (0.7, 0.9)	5.2% (5.0, 5.3)	33.3% (33.2, 33.4)
	Mean	**6.4% (6.1, 6.6)**	**22.9% (22.5, 23.2)**	**143% (143, 144)**	**22.6% (22.1, 23.0)**	**43.3% (42.9, 43.7)**	**119% (119, 120)**
		After 2500 Consumers					
		TS			**UCB**		
		5 Arms	10 Arms	100 Arms	5 Arms	10 Arms	100 Arms
Uplift from 1st externality (GP compared to base algos)	**B(2,9)**	-6.4% (-6.5, -6.2)	-1.6% (-1.9, -1.3)	262% (260, 264)	2.2% (1.9, 2.4)	40.4% (39.7, 41.1)	464% (462, 467)
	B(2,2)	0.3% (0.1, 0.4)	3.4% (3.2, 3.5)	31.4% (31.2, 31.6)	1.0% (0.9, 1.1)	5.0% (4.8, 5.1)	35.2% (35.0, 35.4)
	B(9,2)	-0.5% (-0.6, -0.5)	0.0% (0.0, 0.1)	8.8% (8.7, 8.9)	0.1% (0.0, 0.1)	1.3% (1.3, 1.4)	12.5% (12.4, 12.6)
	Mean	**-2.1% (-2.2, -2.0)**	**0.6% (0.5, 0.8)**	**48.4% (48.2, 48.6)**	**1.0% (0.9, 1.1)**	**11.1% (11.0, 11.3)**	**54.7% (54.5, 54.9)**
Uplift from 2nd externality (GP-M compared to GP algos)	**B(2,9)**	10.9% (10.6, 11.1)	17.4% (17.1, 17.8)	14.9% (14.6, 15.2)	18.0% (17.6, 18.5)	27.6% (27.1, 28.1)	29.4% (28.9, 30.0)
	B(2,2)	1.0% (0.9, 1.1)	0.7% (0.5, 0.8)	0.9% (0.7, 1.0)	0.4% (0.3, 0.5)	0.3% (0.2, 0.5)	0.3% (0.1, 0.4)
	B(9,2)	0.2% (0.2, 0.3)	0.3% (0.2, 0.3)	0.3% (0.2, 0.3)	0.1% (0.1, 0.2)	0.2% (0.1, 0.2)	-0.1% (-0.1, 0.0)
	Mean	**3.7% (3.6, 3.8)**	**5.5% (5.4, 5.6)**	**4.8% (4.7, 4.9)**	**5.3% (5.1, 5.4)**	**7.7% (7.5, 7.8)**	**7.8% (7.7, 7.9)**
Uplift from both externalities (GP-M compared to base algos)	**B(2,9)**	3.8% (3.6, 4.0)	15.4% (15.2, 15.6)	315% (313, 318)	20.5% (20.0, 21.0)	78.9% (78.1, 79.7)	629% (627, 632)
	B(2,2)	1.3% (1.1, 1.4)	4.0% (3.9, 4.2)	32.5% (32.3, 32.7)	1.4% (1.3, 1.6)	5.3% (5.1, 5.5)	35.6% (35.4, 35.8)
	B(9,2)	-0.3% (-0.4, -0.3)	0.3% (0.2, 0.4)	9.0% (8.9, 9.1)	0.2% (0.2, 0.3)	1.5% (1.4, 1.5)	12.4% (12.3, 12.5)
	Mean	**1.5% (1.4, 1.6)**	**6.2% (6.1, 6.3)**	**55.5% (55.4, 55.7)**	**6.3% (6.2, 6.4)**	**19.6% (19.5, 19.8)**	**66.8% (66.6, 66.9)**

Notes. The table provides mean uplifts (averaged across 1000 simulations) along with their corresponding 99% confidence intervals, calculated using a paired t-test. The means are weighted.

externality is most influenced by the number of arms, the uplift from the second externality is primarily affected by the underlying distribution. That is, the two externalities lead to improvements in different scenarios, such that the combined improvement from adding both greatly exceeds their individual contributions.

After 2500 consumers, the benefit of incorporating the first informational externality into both TS and UCB increases with the number of arms across all three distributions. Averaged across the distributions, the uplift for TS is −2.1% for 5 arms, 0.6% for 10 arms, and 48.4% for 100 arms. For UCB, the corresponding uplifts are 1.0%, 11.1%, and 54.7%. For 100 arms, a common pattern for both TS and UCB emerges: the uplift sharply decreases as the optimal price increases, shifting from the right-skewed Beta(2,9) to the left-skewed Beta(9,2). These differences are substantial, with uplifts exceeding 200% for Beta(2,9) but dropping to just 9%–13% for Beta(9,2). This pattern persists for UCB across all numbers of arms, whereas for TS, the first externality actually decreases profits in the Beta(2,9) case for both 5 and 10 arms.

For the second informational externality, the uplift patterns are consistent within the TS and UCB families of algorithms, specifically for GP-TS to GP-TS-M and GP-UCB to GP-UCB-M. Across varying numbers of arms, the uplifts remain stable, ranging from 3.7% to 5.5% for the TS family and 5.3% to 7.8% for the UCB family. However, the uplifts vary significantly between distributions, with most of the gains concentrated in the Beta(2,9) case; they drop to under 1% for Beta(2,2) and approach 0% for Beta(9,2).

For 500 consumers, the uplift patterns are similar to those observed for 2500 consumers but tend to be more pronounced. This is because comparative gains from algorithms often occur in the early rounds; over time, all algorithms eventually converge to the optimal price. This also implies that informational externalities are broadly valuable, regardless of whether the manager operates with a low experimentation budget (500 consumers) or a relatively high one (2500 consumers).

6.1.3. Mechanism: Investigating the Prices Chosen by Algorithms To understand why algorithms vary in performance, we examine the set of prices (arms) selected by each algorithm. Figure 5 presents three sets of three panels. Each graph includes both a left and a right y-axis. The left y-axis corresponds to the blue bar plots, which show the percentage of time each price was chosen. The right y-axis corresponds to the red horizontal lines, which represent the proportion of optimal rewards obtainable by selecting that price. The highest red line is further marked with a black dot, indicating the price that achieved the maximum reward within the price set as well as its percentage of the true optimal.

The value of the first informational externality (including a GP) increases with the number of arms, with the largest gains observed when there were 100 arms, while for 5 arms,

Figure 5 Histogram of Prices Played

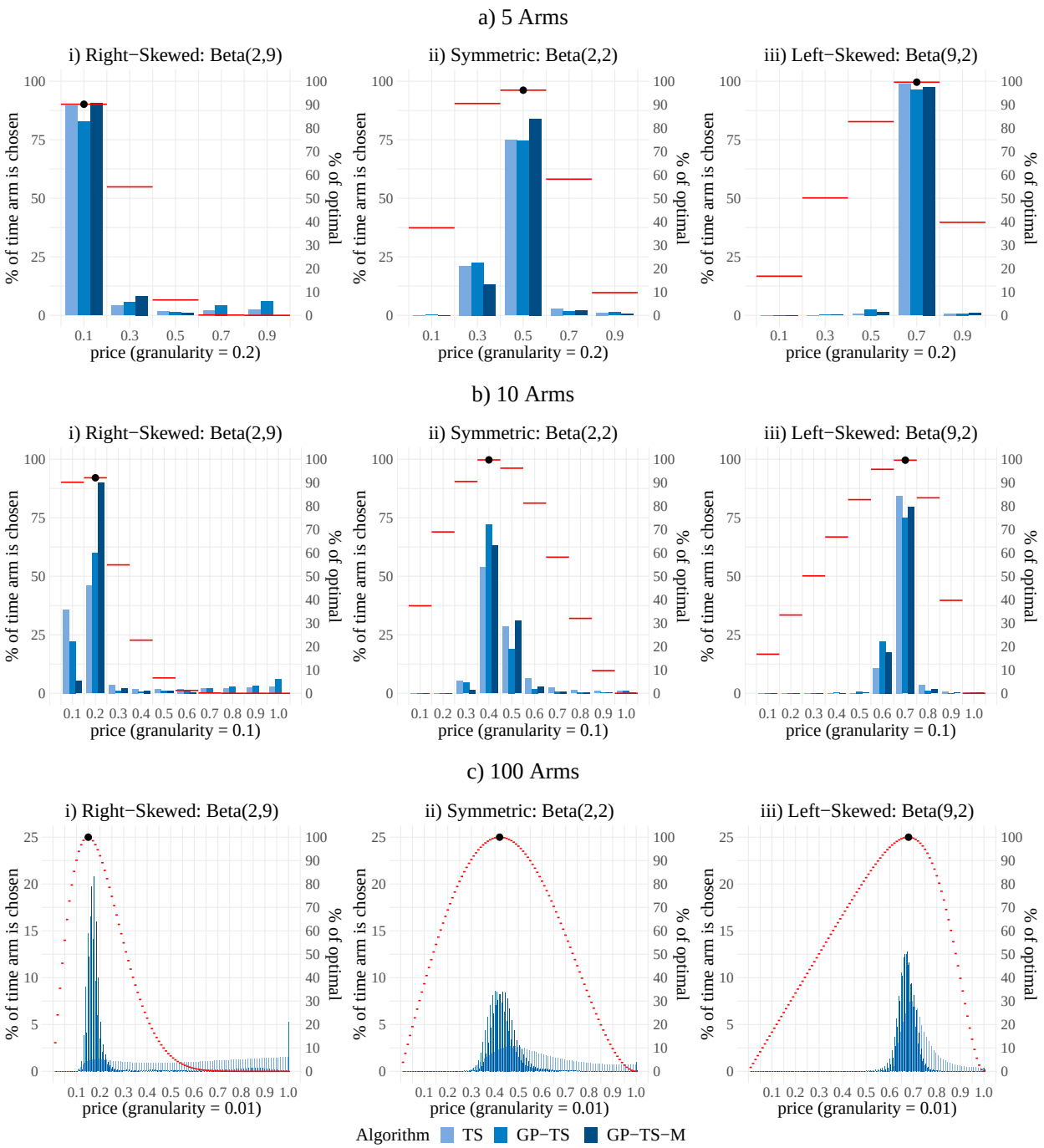

Notes. Each subfigure has two y-axes, with price as the common x-axis. The left y-axis corresponds to the bar plots and represents the % of time each arm is chosen (based on 2500 consumers, averaged over 1000 simulations). The right y-axis corresponds to the red horizontal lines, which indicate the % of the true optimal reward obtainable at each corresponding price. The black dot marks the price that is optimal within the price set.

the gains were negligible or even negative. The mechanism behind this becomes clear when comparing the top row (5 arms) with the bottom row (100 arms) of Figure 5. Since TS does not account for dependence across arms, it must learn the reward for each price individually,

requiring extensive testing of each price. In contrast, GP-TS can pool information across many low-performing arms, enabling it to focus on areas with higher rewards more quickly without repeatedly testing each price. As the number of arms increases, these advantages become substantial. However, with just 5 arms, TS can learn the reward distribution for each price relatively quickly and may even outperform GP-TS. This is because, as discussed in Appendix EC.8, the exploration losses from larger noise bounds in the GP can outweigh the benefits of sharing information across arms.

Meanwhile, for the second informational externality, the largest gains occurred in the Beta(2,9) case, with positive uplifts diminishing as we move to the Beta(2,2) and Beta(9,2) cases. In the top-left panel (5 arms, right-skewed), all algorithms play the optimal price of 0.1 the majority of the time. However, both TS and GP-TS play prices 0.7 and 0.9 with a non-negligible frequency, whereas GP-TS-M almost never selects these prices. Since these arms provide nearly zero reward, playing them is quite costly, which highlights the superior performance of GP-TS-M.

To understand why this occurs, recall that profit is demand scaled by price, meaning that even if demands are learned equally across prices, uncertainty bounds around profits are increasing with price. Algorithms that do not consider monotonicity (such as TS and GP-TS) must invest significant resources to determine whether high prices are suboptimal. As monotonicity requires each demand curve to be monotonically decreasing, it eliminates many possible demand curves that TS and GP-TS cannot disregard. Specifically, it can lead to gains by excluding from consideration demand curves that upward-slope at high prices when the true optimal is a low price. Thus, with minimal data, monotonicity effectively reduces the need to explore high-noise, low-profit regions, demonstrating its value.

This advantage, however, applies only when the optimal price is low. Because lower prices have smaller reward bounds, other algorithms can also quickly dismiss low-profit, low-price arms; for example, the left-skewed panels of Figure 5 show that all of the algorithms rarely played prices below 0.5. Ultimately, the advantage from incorporating the second informational externality diminishes as the optimal price within the price set increases, although it remains positive across all simulations we ran.

6.1.4. Robustness: Alternative WTP Distributions We also conduct several analyses to assess the robustness of the method developed here. First, in Appendix EC.5, we test our method in an empirical setting using a demand curve estimated from field data. In

this setting, the optimal price was low within the price set considered, and the results accordingly aligned with the Beta(2,9) case for 5, 10, and 100 arms. This lends credence to our main analysis and demonstrates the practical value and applicability of the method.

Next, since the GP-based method requires continuity of the demand curve, we consider cases where the demand curve has discontinuities at known prices – specifically, left-digit bias (Thomas and Morwitz 2005), where consumers perceive a larger price increase when the left-digit changes (e.g., from \$1.99 to \$2.00 is perceived as greater than a one-cent increase). We find that even in this situation, the informational externalities improve performance (see Appendix EC.6). However, if the left-digit bias is large enough, it may be more effective for a firm to use only the prices immediately preceding the discontinuities as the price set rather than adopting a finer price granularity.

Finally, to examine whether the proposed bandit algorithms provide a long-run or persistent advantage, we explore the case of time-varying (seasonal) demand in Appendix EC.7, where we introduce an unknown demand shock each period. Once again, we find that informational externalities, especially monotonicity, significantly enhance long-term profits. Notably, learning is so efficient that, if the shocks are large enough, GP-TS-M can achieve higher profits by restarting the bandit experiment at each shock rather than relying on prior data. For the other algorithms tested, however, the start-up cost outweighed the gains from more accurately learning the demand curve.

7. Conclusion and Future Research

We have proposed a method for efficient and robust learning of the relevant portion of the demand curve by using reinforcement learning informed by microeconomic principles. In particular, we introduced a new approach that incorporates monotonicity into multi-armed bandits.

Notably, our algorithm outperformed baseline methods across a variety of scenarios, achieving significant gains in both the short and long term. As expected, the majority of the improvement over baseline methods occurs in the early rounds of experimentation, as all algorithms eventually converge to the optimal. This makes our method particularly beneficial for managers with limited time for experimentation. By reducing the required experimentation time, our approach makes price experimentation more feasible, minimizing potential monetary losses and limiting consumer impact. Additionally, our method enables testing a finer grid of prices, allowing firms to evaluate prices closer to the true optimal.

This not only increases gains during the experiment but can also lead to long-term profit improvements when a near-optimal price is adopted after the experiment concludes.

There are several avenues to extend this research. First, the method could be adapted to settings involving multiple units purchased or multiple products, where consumer choices for one product inform the valuation distribution of related products. Second, applying the method to competitive environments, where competitors are experimenting with price levels and demand responses, would be a valuable extension. More broadly, efficiently learning unknown demand curves with minimal experimental impact remains a significant challenge across many markets. This research contributes to addressing this challenge by closely integrating theory with algorithm development.

Funding and Competing Interests

All authors certify that they have no affiliations with or involvement in any organization or entity with any financial interest or non-financial interest in the subject matter or materials discussed in this manuscript. The authors have no specific funding to report.

References

Aghion P, Bolton P, Harris C, Jullien B (1991) Optimal learning by experimentation. *The review of economic studies* 58(4):621–654.

Agrawal R (1995) Sample mean based index policies by o (log n) regret for the multi-armed bandit problem. *Advances in Applied Probability* 27(4):1054–1078.

Agrawal S, Goyal N (2012) Analysis of thompson sampling for the multi-armed bandit problem. *Conference on learning theory*, 39–1.

Ariely D (2010) Why businesses don't experiment. *Harvard business review* 88(4).

Auer P (2002) Using confidence bounds for exploitation-exploration trade-offs. *Journal of Machine Learning Research* 3(Nov):397–422.

Auer P, Cesa-Bianchi N, Fischer P (2002) Finite-time analysis of the multiarmed bandit problem. *Machine learning* 47(2-3):235–256.

Bayati M, Hamidi N, Johari R, Khosravi K (2020) Unreasonable effectiveness of greedy algorithms in multi-armed bandit with many arms. *Advances in Neural Information Processing Systems* 33:1713–1723.

Bergemann D, Schlag KH (2008) Pricing without priors. *Journal of the European Economic Association* 6(2-3):560–569.

Besbes O, Zeevi A (2009) Dynamic pricing without knowing the demand function: Risk bounds and near-optimal algorithms. *Operations Research* 57(6):1407–1420.

Botev Z, Belzile L (2021) *TruncatedNormal: Truncated Multivariate Normal and Student Distributions*. URL `https://CRAN.R-project.org/package=TruncatedNormal`, r package version 2.2.2.

Chapelle O, Li L (2011) An empirical evaluation of thompson sampling. *Advances in neural information processing systems*, 2249–2257.

Chatterjee S, Sen S (2021) Regret minimization in isotonic, heavy-tailed contextual bandits via adaptive confidence bands. URL `https://arxiv.org/abs/2110.10245`.

Chen Q, Jasin S, Duenyas I (2019) Nonparametric self-adjusting control for joint learning and optimization of multiproduct pricing with finite resource capacity. *Mathematics of Operations Research* 44(2):601–631.

Cheshire J, Ménard P, Carpentier A (2020) The influence of shape constraints on the thresholding bandit problem. *Conference on Learning Theory*, 1228–1275 (PMLR).

Ching AT, Osborne M (2020) Identification and estimation of forward-looking behavior: The case of consumer stockpiling. *Marketing Science* 39(4):707–726.

Chou C, Kumar V (2024) Estimating demand for subscriptions: Identifying willingness to pay without price variation. *Marketing Science (Forthcoming)* .

Chowdhury SR, Gopalan A (2017) On kernelized multi-armed bandits. *International Conference on Machine Learning*, 844–853 (PMLR).

Cohen SN, Treetanthiploet T (2020) Asymptotic randomised control with applications to bandits. *arXiv preprint arXiv:2010.07252* .

Dann C, Mansour Y, Mohri M, Sekhari A, Sridharan K (2022) Guarantees for epsilon-greedy reinforcement learning with function approximation. *Proceedings of the 39th International Conference on Machine Learning*, volume 162 of *Proceedings of Machine Learning Research*, 4666–4689 (PMLR).

Duvenaud D (2014) *Automatic model construction with Gaussian processes*. Ph.D. thesis.

Erdem T, Keane MP (1996) Decision-making under uncertainty: Capturing dynamic brand choice processes in turbulent consumer goods markets. *Marketing science* 15(1):1–20.

Ferreira KJ, Simchi-Levi D, Wang H (2018) Online network revenue management using thompson sampling. *Operations research* 66(6):1586–1602.

Filippi S, Cappe O, Garivier A, Szepesvári C (2010) Parametric bandits: The generalized linear case. *Advances in neural information processing systems* 23.

Furman J, Simcoe T (2015) The economics of big data and differential pricing. *The White House President Barack Obama* .

Gittins J (1974) A dynamic allocation index for the sequential design of experiments. *Progress in statistics* 241–266.

Goldberg PW, Williams CK, Bishop CM (1997) Regression with input-dependent noise: A gaussian process treatment. *Advances in neural information processing systems* 10:493–499.

Gordon BR, Zettelmeyer F, Bhargava N, Chapsky D (2019) A comparison of approaches to advertising measurement: Evidence from big field experiments at facebook. *Marketing Science* 38(2):193–225.

Guntuboyina A, Sen B (2018) Nonparametric shape-restricted regression. *Statistical Science* 33(4):568–594.

Handel BR, Misra K (2015) Robust new product pricing. *Marketing Science* 34(6):864–881.

Hanssens DM, Pauwels KH (2016) Demonstrating the value of marketing. *Journal of marketing* 80(6):173–190.

Hauser JR, Urban GL, Liberali G, Braun M (2009) Website morphing. *Marketing Science* 28(2):202–223.

Hendel I, Nevo A (2006) Measuring the implications of sales and consumer inventory behavior. *Econometrica* 74(6):1637–1673.

Hill DN, Nassif H, Liu Y, Iyer A, Vishwanathan S (2017) An efficient bandit algorithm for realtime multivariate optimization. *Proceedings of the 23rd ACM SIGKDD International Conference on Knowledge Discovery and Data Mining*, 1813–1821.

Hoban PR, Bucklin RE (2015) Effects of internet display advertising in the purchase funnel: Model-based insights from a randomized field experiment. *Journal of Marketing Research* 52(3):375–393.

Hoffman M, Brochu E, De Freitas N, et al. (2011) Portfolio allocation for bayesian optimization. *UAI*, 327–336 (Citeseer).

Huang J, Reiley D, Riabov N (2018) Measuring consumer sensitivity to audio advertising: A field experiment on pandora internet radio. *Available at SSRN 3166676* .

Huang Y, Ellickson PB, Lovett MJ (2022) Learning to set prices. *Journal of Marketing Research* 59(2):411–434.

Jindal P, Zhu T, Chintagunta P, Dhar S (2020) Marketing-mix response across retail formats: the role of shopping trip types. *Journal of Marketing* 84(2):114–132.

Kawale J, Bui HH, Kveton B, Tran-Thanh L, Chawla S (2015) Efficient thompson sampling for online matrix-factorization recommendation. *Advances in neural information processing systems*, 1297–1305.

Kersting K, Plagemann C, Pfaff P, Burgard W (2007) Most likely heteroscedastic gaussian process regression. *Proceedings of the 24th international conference on Machine learning*, 393–400.

Lai TL, Robbins H (1985) Asymptotically efficient adaptive allocation rules. *Advances in applied mathematics* 6(1):4–22.

Lambrecht A, Tucker C, Wiertz C (2018) Advertising to early trend propagators: Evidence from twitter. *Marketing Science* 37(2):177–199.

Lei YM, Jasin S, Sinha A (2014) Near-optimal bisection search for nonparametric dynamic pricing with inventory constraint. *Ross School of Business Paper* (1252).

Li Z, Jamieson K, Jain L (2023) Optimal exploration is no harder than thompson sampling. *arXiv preprint arXiv:2310.06069* .

Maatouk H, Bay X (2017) Gaussian process emulators for computer experiments with inequality constraints. *Mathematical Geosciences* 49(5):557–582.

Miao S, Wang Y (2024) Demand balancing in primal-dual optimization for blind network revenue management. URL `https://arxiv.org/abs/2404.04467`.

Micchelli CA, Xu Y, Zhang H (2006) Universal kernels. *Journal of Machine Learning Research* 7(12).

Misra K, Schwartz EM, Abernethy J (2019) Dynamic online pricing with incomplete information using multiarmed bandit experiments. *Marketing Science* 38(2):226–252.

Murray I (2008) Introduction to gaussian processes. *Dept. Computer Science, University of Toronto* .

Nair H (2007) Intertemporal price discrimination with forward-looking consumers: Application to the us market for console video-games. *Quantitative Marketing and Economics* 5(3):239–292.

Oren SS, Smith SA, Wilson RB (1982) Nonlinear pricing in markets with interdependent demand. *Marketing Science* 1(3):287–313.

Pfeffer J, Sutton RI (2006) Evidence-based management. *Harvard business review* 84(1):62.

Rao RC, Bass FM (1985) Competition, strategy, and price dynamics: A theoretical and empirical investigation. *Journal of Marketing Research* 22(3):283–296.

Rebonato R, Jäckel P (2011) The most general methodology to create a valid correlation matrix for risk management and option pricing purposes. *Available at SSRN 1969689* .

Ringbeck D, Huchzermeier A (2019) Dynamic pricing and learning: An application of gaussian process regression. *Available at SSRN 3406293* .

Rothschild M (1974) A two-armed bandit theory of market pricing. *Journal of Economic Theory* 9(2):185–202.

Rubel O (2013) Stochastic competitive entries and dynamic pricing. *European Journal of Operational Research* 231(2):381–392.

Russo D (2016) Simple bayesian algorithms for best arm identification. *Conference on Learning Theory*, 1417–1418 (PMLR).

Russo D, Van Roy B (2014) Learning to optimize via posterior sampling. *Mathematics of Operations Research* 39(4):1221–1243.

Sahni NS, Nair HS (2020) Does advertising serve as a signal? evidence from a field experiment in mobile search. *The Review of Economic Studies* 87(3):1529–1564.

Schwartz EM, Bradlow ET, Fader PS (2017) Customer acquisition via display advertising using multi-armed bandit experiments. *Marketing Science* 36(4):500–522.

Shahriari B, Swersky K, Wang Z, Adams RP, De Freitas N (2015) Taking the human out of the loop: A review of bayesian optimization. *Proceedings of the IEEE* 104(1):148–175.

Simester D, Hu Y, Brynjolfsson E, Anderson ET (2009) Dynamics of retail advertising: Evidence from a field experiment. *Economic Inquiry* 47(3):482–499.

Soysal GP, Krishnamurthi L (2012) Demand dynamics in the seasonal goods industry: An empirical analysis. *Marketing Science* 31(2):293–316.

Srinivas N, Krause A, Kakade SM, Seeger M (2009) Gaussian process optimization in the bandit setting: No regret and experimental design. *arXiv preprint arXiv:0912.3995* .

Strulov-Shlain A (2023) More than a penny's worth: Left-digit bias and firm pricing. *Review of Economic Studies* 90(5):2612–2645.

Thomas M, Morwitz V (2005) Penny wise and pound foolish: the left-digit effect in price cognition. *Journal of Consumer Research* 32(1):54–64.

Thompson WR (1933) On the likelihood that one unknown probability exceeds another in view of the evidence of two samples. *Biometrika* 25(3/4):285–294.

Tirole J (1988) *The theory of industrial organization* (MIT press).

Wang Y, Chen B, Simchi-Levi D (2021) Multimodal dynamic pricing. *Management Science* 67(10):6136–6152.

Williams CK, Rasmussen CE (2006) *Gaussian processes for machine learning*, volume 2 (MIT press Cambridge, MA).

Yu M, Debo L, Kapuscinski R (2016) Strategic waiting for consumer-generated quality information: Dynamic pricing of new experience goods. *Management Science* 62(2):410–435.

Zhang L, Chung DJ (2020) Price bargaining and competition in online platforms: An empirical analysis of the daily deal market. *Marketing Science* 39(4):687–706.

Zhao H, He J, Zhou D, Zhang T, Gu Q (2023) Variance-dependent regret bounds for linear bandits and reinforcement learning: Adaptivity and computational efficiency. *The Thirty Sixth Annual Conference on Learning Theory*, 4977–5020 (PMLR).

Electronic Companion Supplement

EC.1 Gaussian Process Regression

This section provides an overview of Gaussian process regression. Formally, the assumption is that the demand function D is jointly Gaussian-distributed and completely defined by its mean $\mu(p)$ and covariance function $k(p,p')$ such that $D(p) \sim \text{GP}(\mu(p), k(p,p'))$. The mean and covariance function are defined as follows (Williams and Rasmussen 2006):

$$\mu(p) = \mathbb{E}[D(p)] \tag{EC.1}$$

$$k(p,p') = \mathbb{E}[(D(p)-\mu(p))(D(p')-\mu(p'))] \tag{EC.2}$$

For ease of exposition, we set $\mu(p) = 0$.[33] Then, the kernel can be used to compute a covariance matrix $K(P,P)$ containing the covariance between all sets of test points, as well as a covariance matrix (either $K(P,P_t)$ or $K(P_t,P)$) between training and test cases. Then, the joint distribution of the training data P_t and the test points P can be written as follows (equation (2.21) in Williams and Rasmussen (2006)):

$$\begin{pmatrix} y_t \\ D^* \end{pmatrix} \sim \mathcal{N}\left(0, \begin{bmatrix} K(P_t,P_t)+\sigma_y^2 I & K(P_t,P) \\ K(P,P_t) & K(P,P) \end{bmatrix}\right) \tag{EC.3}$$

where $D^* = D(P)$ is a random variable denoting the Gaussian process posterior prediction. It then follows from equations (2.22 - 2.24) in Williams and Rasmussen (2006) that

$$D^*|P_t, y_t, P \sim N(\mu(D^*), \text{Cov}(D^*)) \text{ where} \tag{EC.4}$$

$$\mu(D^*) = K(P,P_t)[K(P_t,P_t)+\sigma_y^2 I]^{-1} y_t \text{ and} \tag{EC.5}$$

$$\text{Cov}(D^*) = K(P,P) - K(P,P_t)[K(P_t,P_t)+\sigma_y^2 I]^{-1} K(P_t,P) \tag{EC.6}$$

Figure EC.1 illustrates a simple example of GP regression. As data is obtained, the space in which the true demand function could live becomes restricted. Accordingly, the range of uncertainty is smaller in areas closer to data points compared to those far away from data points (as shown by the shaded area which represents the 95% confidence intervals at the test points).

[33] If the prior mean function is non-zero, when $D \sim GP(\mu, k)$, the function $D' = D - \mu$ is a zero-mean Gaussian process $D' \sim GP(0,k)$. Hence, using observations from the values of D, one can subtract the prior mean function values to get observations of D', and do the inference on D'. Finally, after obtaining the posterior on $D'(P)$, one can simply add back the prior mean $\mu(P)$ to the posterior mean to obtain the posterior on D.

Figure EC.1 Random Samples from Gaussian Process With and Without Training Data

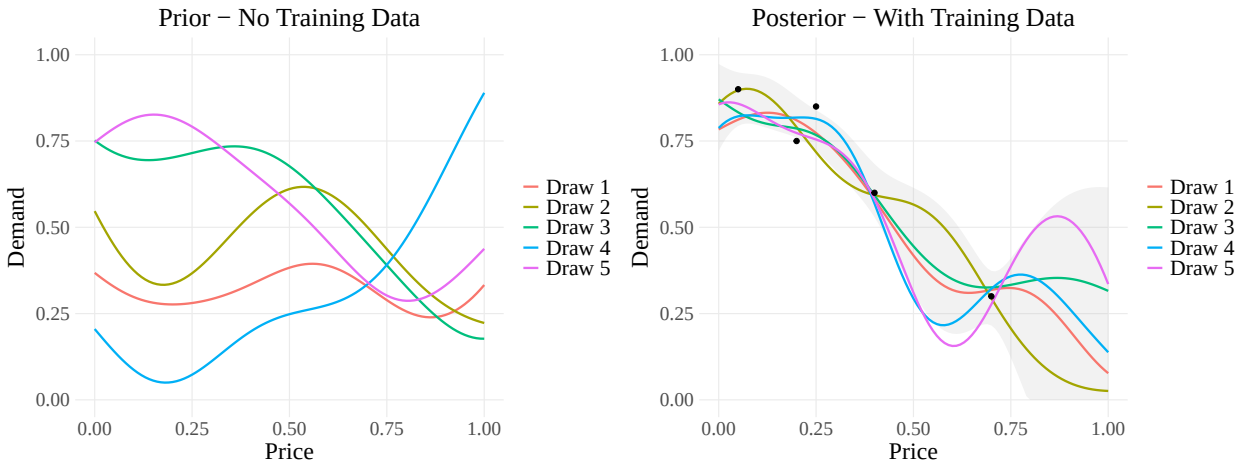

Notes. Lines represent five random draws from the GP in both the prior and the posterior. In the prior, the mean was set to 0.5. For both the prior and posterior, the RBF kernel was used with hyperparameters $l = 0.2, \sigma_f^2 = 0.08, \sigma_y^2 = 0.0016$. There were 101 test points $P = \{0, 0.01, 0.02, ..., 1\}$. The five draws from the posterior distribution are drawn from the GP with training data $P_t = \{0.05, 0.2, 0.25, 0.4, 0.7\}$, and $y_t = \{0.9, 0.75, 0.85, 0.6, 0.3\}$. The shaded area provides the 95% confidence interval at each test point.

EC.2 Computational Issues

A computational issue that arises in fitting a posterior Gaussian process is that matrix inversion is $\mathcal{O}(n^3)$, implying that it does not scale well to larger datasets. Typically, the training data would get larger with every purchase observation (thus depending on t), but we are able to curtail this issue because purchases can only be observed at prices contained within the fixed price set. This means we can set the input training data to be the set of test prices, and the associated output training data to be the observed purchase rates. The only additional adjustment needed is to the noise hyperparameter. As the sample variance scales with the number of observations, the noise hyperparameter is specified accordingly: $\sigma_y^2 = \{0.25/n_{1t}, ..., 0.25/n_{Kt}\}$. This approach means that the computational complexity will not increase as the number of purchase observations increases, but rather is dependent on the size of the initial set of test prices.

Additionally, one common issue when running GP algorithms is floating point precision errors, which can lead to negative eigenvalues, violating the positive semi-definite property of covariance matrices. We follow an approach devised by Rebonato and Jäckel (2011) to obtain the nearest covariance matrix.

EC.3 Implementation of Monotonic GP Bandits

EC.3.1 Basis Function Visualization

Consider an example where $N = 4$ meaning there are 5 equally spaced knots $\{0, \frac{1}{4}, \frac{1}{2}, \frac{3}{4}, 1\}$. Figure EC.2 shows the five basis functions along with their corresponding integrals.

Figure EC.2 Plot of Basis Functions and their Integrals (5 knots)

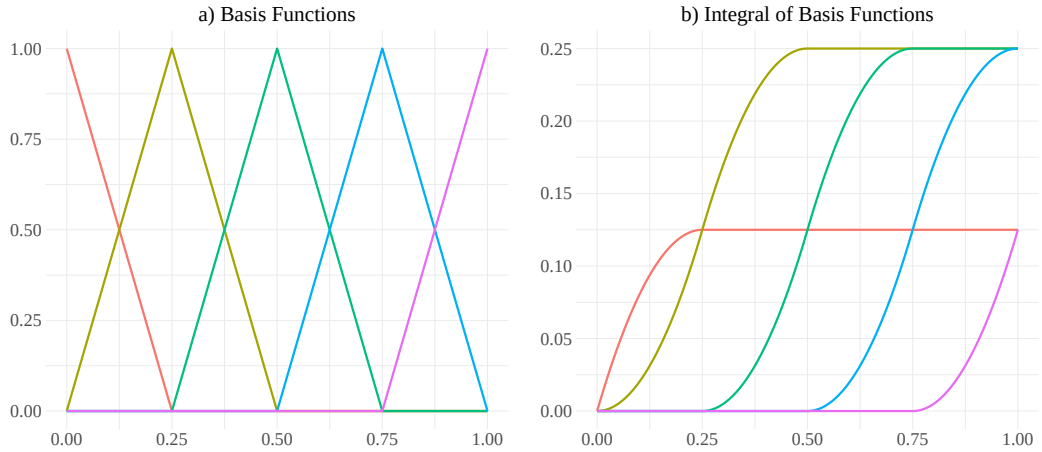

EC.3.2 Derivation of Proposition 1

LEMMA EC.1. *The distance between a continuous function D and its estimate via basis functions $D_N(p) = \sum_{j=0}^{N} D(u_j)h_j(p)$ converges to 0 as $N \to \infty$.*

From Lemma EC.1, a continuous demand function D can be estimated via basis functions as $D(p) \approx \sum_{j=0}^{N} D(u_j)h_j(p)$. Since, by assumption, the derivative of D is also continuous, the same formula can be used to estimate D' as follows:

$$D'(p) \approx \sum_{j=0}^{N} D'(u_j)h_j(p). \tag{EC.7}$$

Additionally, by the Fundamental Theorem of Calculus,

$$D(p) - D(0) = \int_0^p D'(t)\,dt. \tag{EC.8}$$

Substituting (EC.7) into (EC.8) gives

$$D(p) \approx D(0) + \sum_{j=0}^{N} D'(u_j) \int_0^p h_j(t)\,dt. \quad \square \tag{EC.9}$$

EC.3.3 Gaussian Process – Estimation of Derivatives and Intercept

The basis function method requires the estimation of the intercept and the derivatives at each of the prices in the consideration set. More formally, the goal is to estimate the posterior mean and covariance for $\{D(0), D'(p_1), ..., D'(p_k)\}$. Temporarily ignoring the intercept, the key is that the derivatives of a GP are also a GP. This means that D'^*, the posterior vector of derivatives of D^*, is

$$D'^* \sim N\left(\frac{d}{dp}\mu(D^*), \frac{d}{dp}\,\mathrm{Cov}(D^*)\right) \tag{EC.10}$$

Note as the values of D^* are only at our test points P, then the derivative only needs to be calculated with respect to P. This means that to estimate the posterior mean and covariance for $\{D(0), D'(p_1), ..., D'(p_k)\}$, the only necessary changes are to calculate the derivatives of the kernel function with respect to the test points.

We compute the partial derivatives of the kernel with respect to the prices as follows:

$$\frac{\partial k(p_i^*, p_j)}{\partial p_i^*} = \frac{\sigma_f^2}{l^2}(p_j - p_i^*)\exp\left(\frac{-(p_i^* - p_j)^2}{2l^2}\right) \tag{EC.11}$$

$$\frac{\partial k(p_i, p_j^*)}{\partial p_j^*} = \frac{\sigma_f^2}{l^2}(p_i - p_j^*)\exp\left(\frac{-(p_i - p_j^*)^2}{2l^2}\right) \tag{EC.12}$$

$$\frac{\partial^2 k(p_i^*, p_j^*)}{\partial p_i^* \partial p_j^*} = \frac{\sigma_f^2}{l^4}\left(l^2 - (p_i^* - p_j^*)^2\right)\exp\left(\frac{-(p_i^* - p_j^*)^2}{2l^2}\right) \tag{EC.13}$$

EC.4 Bounds for Joint Monotonic Algorithm

Consider a setting where $\mathcal{P} = \{p_1 \le p_2 \le \cdots \le p_d\}$ are a subset of prices that we choose as knots. We consider a Gaussian process for which draws are C^1 almost surely, and consider the joint distribution over draws f, f'. We define the set of monotonic functions,

$$M\{f \in C^1([0,1]) : f'(x) \le 0, x \in [0,1]\}.$$

Ideally we would like to restrict draws of our GP to M, but in general, since we can only evaluate our GP at a finite set of points, we instead insist that our function is monotonic at the set of knots,

$$M(\mathcal{P}) = \{f(\in C^1[0,1] : f'(p) \le 0, p \in \mathcal{P}\}$$

We denote the joint prior distribution over the function and the derivative $\Pi_0 = GP([0,0], K|\mathcal{M}(P))$, where K is the appropriate kernel.

Let $p^* = \arg\max_{p \in P} f(p)$ — note that since f is drawn from the underlying prior, p^* is a random variable. We define the Bayesian regret of our policy

$$BR_T = \sum_{t=1}^{T} \mathbb{E}[p^* f(p^*) - p_t f(p_t)]$$

where the expectation is over draws from the prior, reward noise, and any internal randomness of the algorithm.

Throughout the following, we refer to the truncated distribution as Π_t, and the untruncated distribution $GP([\mu_t, \mu_t'], K_t)$ as $\Pi_{t,u}$. Let the induced probability laws and expecation, with respect to the measure conditioned on the history $\mathcal{H}_t = \{(p_s, r_s)\}_{s=1}^t$, be $\mathbb{P}_t, \mathbb{E}_t$, and for the untruncated version, $\mathbb{P}_{t,u}, \mathbb{E}_{t,u}$. Critically we make the following assumption:

Assumption 1. The probability of returning a function monotonic on the knots is bounded below, i.e., there exists $c \geq 0$ such that

$$\mathbb{P}_{t,u}(f_t, f_t' \in \mathcal{M}(P)) \geq c, \forall t \geq 1$$

Remark: Note that $P_{t,u}(f_t'(P) \geq 0)$ is equivalent to $\mathbb{P}_{D_t}(y \geq 0)$ for $x, y \sim N([\mu_t(P), \mu_t'(P)], K)$. This is an integral of a multivariate Gaussian over an open set. Since $f'(P) \geq 0$ by definition of the prior, if $\mu'(P) \to f'(P)$, we should expect this probability to actually increase with t. We discuss this further below.

THEOREM EC.1. *The Bayes Regret of Joint Algorithm is bounded by*

$$\begin{aligned} BR_t &\leq \mathbb{E}\left[\sqrt{\sum_{t=1}^{\infty} p_t^2}\right] \sqrt{\gamma_T \log(1+\sigma_0^{-2}) \log\left(\frac{T^2|A|}{\sqrt{2\pi}}\right)} + E_T + 1 \\ &\leq \sqrt{T\gamma_T \log(1+\sigma_0^{-2}) \log\left(\frac{T^2|A|}{\sqrt{2\pi}}\right)} + E_T + 1 \end{aligned}$$

where $E_T = \sum_{t=1} \mathbb{E}[\mu_t(p^*) - \mathbb{E}_t[f_t(p^*)]]$ *and* γ_T *is the mutual information of the Gaussian process (Srinivas et al. 2009).*

Interpreting the Regret: We remark that when $S = \mathbb{R}^d$, $\mathbb{E}_t[f(p^*)] = \mu_{t-1}(p^*)$ so E_T is 0. And so the final regret is of the form $O(\sqrt{\gamma_T T \log(T|P|)})$. Note that this regret is independent of the underlying constraint set.

To understand the impact of the underlying constraint set, we focus on the path-dependent regret term $\sum_{t=1}^{T} p_t^2$. In general, this quantity is less than the maximum price played times T, and is a tighter regret result compared to existing works.

We remark that the looseness in this result is primarily due to using loose tail bounds that do not effectively account for the constraint set. Future work could examine different and potentially tighter bounds.

Discussion of Assumption 1 and E_T*.* By Lemma EC.2,

$$\begin{aligned} \mu_t(p^*) - \mathbb{E}_t[f(p^*)] &\leq \mu_t(p^*) - \mathbb{E}_{t,u}[f(p^*)\mathbf{1}\{f \in M\}] \\ &\leq \mathbb{E}_{t,u}[f(p^*) - f(p^*)\mathbf{1}\{f \in M\}] \\ &\leq \mathbb{E}_{t,u}[f(p^*)(1 - \mathbf{1}\{f \in M\})] \\ &\leq \mathbb{E}_{t,u}[f(p^*)\mathbf{1}\{f \notin M\})] \end{aligned}$$

We define $\theta_0 = [f, f'] \sim \Pi_0$ to be the true parameters drawn from the prior, then existing results in the finite-dimensional bandit setting (Li et al. 2023, Russo 2016). We expect

$$\mathbb{P}_{t,u}(\mathbf{1}(f \notin M)) \approx e^{-t \min_{\theta \in M^c} \|\theta_0 - \theta\|^2_{K_t/t}}$$

In particular, if we can guarantee that $\|\theta_0 - \theta\|^2_{K_t/t}$ is bounded below (perhaps by sampling a uniform price $1/\sqrt{t}$ of the time), we see that the probability of not sampling a monotonic function decreases exponentially in time. This argument in particular implies that E_t should be finite.

Proof. We begin with the following lemma linking a distribution with its truncated version.

LEMMA EC.2. *Let $p(x)$ be a distribution on $\mathbb{R}^d$. Let $S \subset \mathbb{R}^d$. Define the truncated pdf on $\mathbb{R}^d$, $p_S(x) = \mathbf{1}\{x \in S\}p(x)/\mu(S)$ where $\mu(S) = \int_{x \in S} p(x)$. Then given an event $E \subset \mathbb{R}^d$,*

$$\mathbb{P}_p(\mathbf{1}\{E \cap S\}) \leq \mathbb{P}_{p_S}(E) \leq \frac{1}{\mu(S)} \mathbb{P}_p(E)$$

and given a function $f(x) : \mathbb{R}^d \to \mathbb{R}$

$$\mathbb{E}_{p_S}(f(x)) \leq \frac{1}{\mu(S)} \mathbb{E}_p(f(x))$$

T he lower bound is immediate since $\mu(S) \leq 1$.

$$\begin{aligned}
\mathbb{P}_{p_S}(E) &= \int_{x \in \mathbb{R}^d} \mathbf{1}\{x \in E\}\mathbf{1}\{x \in S\}p(x)/\mu(S) \\
&= \frac{1}{\mu(S)} \int_{x \in \mathbb{R}^d} \mathbf{1}\{x \in E\}\mathbf{1}\{x \in S\}p(x) \\
&\leq \frac{1}{\mu(S)} \int_{x \in \mathbb{R}^d} \mathbf{1}\{x \in E\}p(x) \\
&\leq \frac{1}{\mu(S)} \mathbb{P}_p(E)
\end{aligned}$$

The result on expectations is almost immediate.

Define $U_t(p) := \mu_{t-1}(p) + \beta_{t-1}^{1/2}\sigma_{t-1}(p)$ where $\beta_t = \log(t^2 c^{-1}|P|/\sqrt{2\pi})$. Note that, conditioned on $\mathcal{H}_t$, the optimal action p^* and the action p_t selected by posterior sampling are identically distributed by Fact 5 (see below). In addition, U_t is deterministic conditioned on the history, so, $\mathbb{E}_t[U_t(p^*)] = \mathbb{E}_t[U_t(A_t)]$. Therefore,

$$\mathbb{E}[p^* f(p^*) - p_t f(p_t)] = \mathbb{E}[\mathbb{E}_t[p^* f(p^*) - p_t f(p_t)]]$$

$$
\begin{aligned}
&= \mathbb{E}[\mathbb{E}_t[p_t U_t(p_t) - p^* U_t(p^*) + p^* f(p^*) - p_t f(p_t)]] \\
&= \mathbb{E}[\mathbb{E}_t[p_t U_t(p_t) - p_t f(p_t)] + \mathbb{E}_t[p^* f(p^*) - p^* U_t(p^*)]] \\
&= \mathbb{E}[p_t U_t(p_t) - p_t f(p_t)] + \mathbb{E}[p^* f(p^*) - p^* U_t(p^*)].
\end{aligned}
$$

Thus, we see that we can bound the Bayes-Regret as

$$
BR(T) \leq \sum_{t=1}^{T} \mathbb{E}[p_t U_t(p_t) - p_t f(p_t)] + \sum_{t=1}^{T} \mathbb{E}[p^* f(p^*) - p^* U_t(p^*)] \tag{EC.14}
$$

$$
\tag{EC.15}
$$

We now focus on the first term,

$$
\begin{aligned}
p_t U_t(p_t) - p_t f(p_t) &= p_t U_t(p_t) - p_t \mu_t(p_t) + p_t \mu_t(p_t) - p_t f(p_t) \\
&= \mathbb{E}[p_t U_t(p_t) - p_t \mu_t(p_t)] + p_t \mu_t(p_t) - p_t f(p_t) \\
&\leq p_t \beta_t^{1/2} \sigma_t(p_t) + p_t \mu_t(p_t) - p_t f(p_t) \\
&\leq p_t \beta_t^{1/2} \sigma_t(p_t) + \mu_t(p_t) - f(p_t)
\end{aligned}
$$

Next,

$$
\sum_{t=1}^{T} p_t \beta_t^{1/2} \sigma_t(p_t) \leq \sqrt{\beta_T \sum_{t=1}^{\infty} p_t^2} \sqrt{\sum_{t=1}^{\infty} \sigma_t^2(p_t)} \qquad \text{(Cauchy-Schwartz)}
$$

A standard argument (see Srinivas et al. (2009)) shows that

$$
\sum_{t=1}^{\infty} \sigma_t^2(p_t) \leq \frac{\gamma_T}{\log(1+\sigma^{-2})}
$$

Finally, we bound the second term of EC.14

$$
\begin{aligned}
\sum_{t=1}^{T} E[p^* f(p^*) - p^* U_t(p^*)] &\leq \sum_{t=1}^{\infty} \sum_{p \in P} \mathbb{E}_t[\mathbf{1}\{f(p) - U_t(p) \geq 0\}(f(p) - U_t(p))] \\
&\leq \sum_{t=1}^{\infty} \sum_{p \in P} \frac{1}{\mathbb{P}_{t,u}(M)} \mathbb{E}_{t,u}[\mathbf{1}\{f(p) - U_t(p) \geq 0\}(f(p) - U_t(p))] \\
&\leq \sum_{t=1}^{\infty} \sum_{p \in P} \frac{1}{c} \mathbb{E}_{t,u}[\mathbf{1}\{f(p) - U_t(p) \geq 0\}(f(p) - U_t(p))]
\end{aligned}
$$

Now, in the untruncated distribution, $\mathbb{E}_{t,u}[f(p) - U_t(p)] = -\beta_t^{1/2}\sigma_t^2(p)$, which is negative. Thus, using standard tail bounds Russo and Van Roy (2014),

$$\sum_{t=1}^{T} E[p^* f(p^*) - p^* U_t(p^*)] \leq \frac{1}{c}\sum_{t=1}^{\infty} \frac{\sigma_t(p)}{\sqrt{2\pi}} e^{-\beta/2}$$
$$\leq \frac{1}{c}\sum_{t=1}^{\infty} \frac{\sigma_t(p)}{t^2|P|c^{-1}} \leq 1$$

The result follows from combining all the terms.

EC.5 Field Data

To further show the applicability and value of our methods when used with real world data, we tested out the algorithms on field data. The data comes from an empirical study of demand for a music streaming subscription service, where the distribution of WTP for a monthly plan is estimated (Chou and Kumar 2024; see Figure 2 on page 15 of that paper). We normalize the data by setting the price $p' = \frac{p}{1000}$ from their WTP distribution, which normalizes the prices to be in $[0, 1]$.

From this WTP distribution, we are able to run the bandit algorithms using the same setup as in the simulations, but just by replacing the simulated WTP curve with the one derived empirically from field data. As the optimal price is relatively low price (0.21) within the set of prices tested, if the trend from the main results replicates, we would expect similar trends in uplifts from the informational externalities as in the Beta(2,9) case.

We find that the results are very consistent with those obtained for Beta(2,9) in the main simulations. The first informational externality (continuity implemented by GP) is negative for 5 arms, but positive for 10, and highly beneficial in the case of 100 arms. The second informational externality (implemented by specifying monotonicity) is positive for all the sets of arms, and is very consistent in terms of the improvement it offers. Overall, the results point to the validity and value of the method in practical applications.

EC.6 Discontinuous Demand: Left-Digit Bias

We next discuss the case where consumers may be affected by left-digit bias. This is a phenomena where the demand function is discontinuous when the left-digit of a price changes (for example, from \$1.99 to \$2.00) as consumers perceive a larger magnitude in the price change than just one cent (Thomas and Morwitz 2005). For example, Strulov-Shlain (2023) empirically found that consumers responded to a one-cent increase from a

Figure EC.3 Place Holder - Will Update

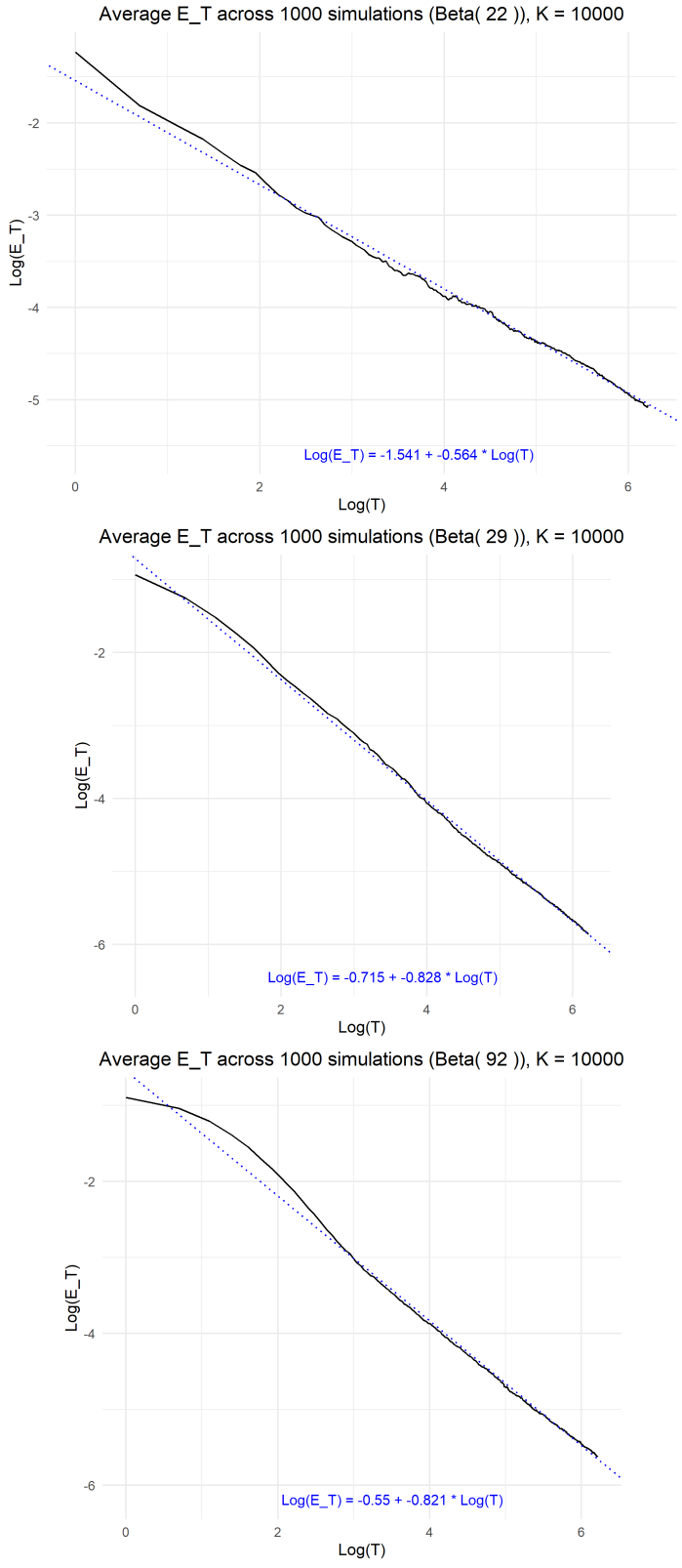

Notes

Figure EC.4 Field Data: Cumulative Percent of Optimal Rewards (Profits)

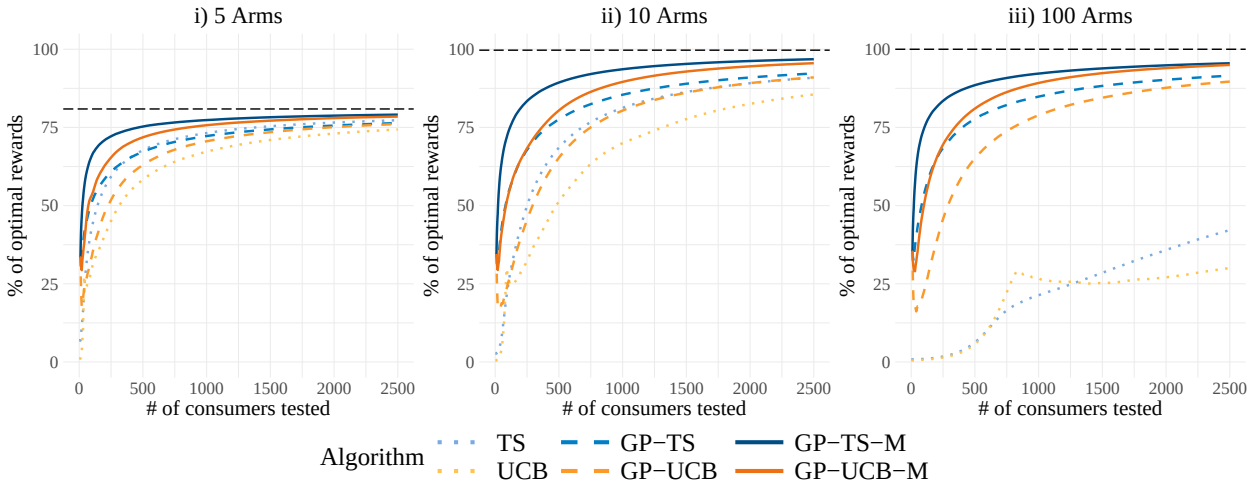

Notes. The lines are the means of the cumulative expected percentage of optimal rewards across the 1000 simulations. The black horizontal line represents the maximum obtainable given the price set, while 100% represents the true optimal given the underlying distribution. The true optimal price is 0.21.

ninety-nine-ending price (leading to a change in the left-digit) as if it were a twenty-cent increase. This is an important case to test as GP-based models rely on continuity and so may struggle with discontinuities.

To be consistent with prior literature, we discretize our continuum of prices $[0,1]$ into 1000 prices and set discontinuities to occur when the left-most significant digit changes (i.e., 0.099 to 0.100, 0.199 to 0.200, etc.). This allows for the left-digit effect to occur between prices ending in ninety-nine and zero. To specify the size of the of discontinuities, we measured the difference in demand between two consecutive prices whenever the left-digit changes and then multiplied it by a scale factor γ. For example, if $\gamma = 20$, then the discontinuity gap would be 20 times larger than usual (equivalent to Strulov-Shlain (2023) where consumers treat a one cent increase from a ninety-nine ending price as if it were a twenty-cent increase). We then rescale the continuous portion of the original demand curve to accommodate these gaps. In our simulations, we used demand curves (Figure EC.5) obtained from the three underlying WTP distributions Beta(2,9), Beta(2,2), and Beta(9,2) adjusted with $\gamma = 10$ (low left-digit bias) and $\gamma = 30$ (high left-digit bias). These two cases provide generous bounds of the estimates of the left-digit bias from Strulov-Shlain (2023).

In our simulations, we used demand curves (Figure EC.5) obtained from the three underlying WTP distributions Beta(2,9), Beta(2,2), and Beta(9,2) adjusted with $\gamma = 10$ (low left-digit bias) and $\gamma = 30$ (high left-digit bias). These two cases provide generous bounds of the estimates of the left-digit bias from Strulov-Shlain (2023).

Figure EC.5 Left-Digit Demand Curves

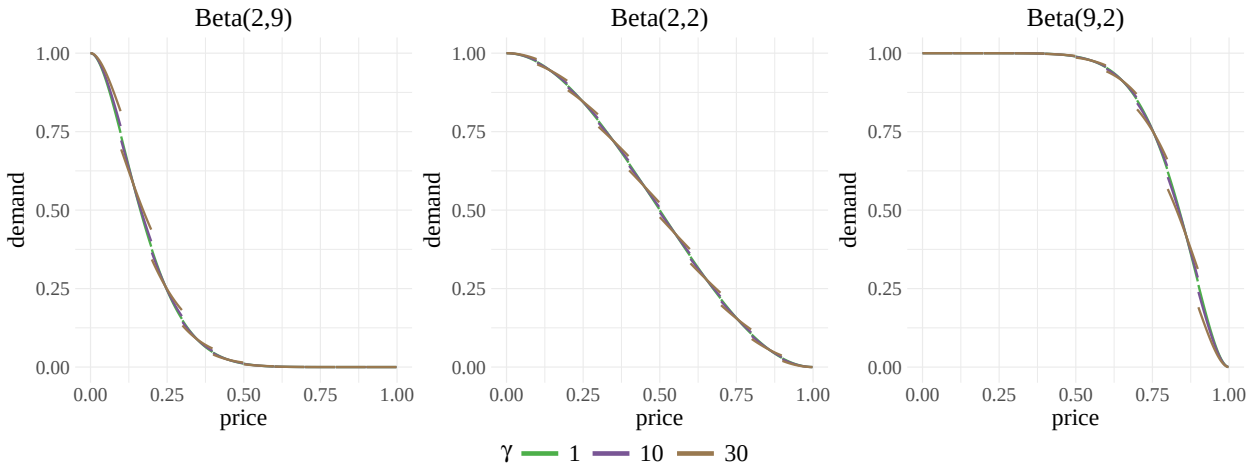

Notes. Price is discretized at a level of 0.001 from 0 to 1 with left-digit discontinuities happening every 0.01. $\gamma = 1$ provides the base case where there is no left-digit bias (there are still "discontinuities" as a result of the discretization of the price). $\gamma = 10$ represents a case of low left-digit bias where the discontinuity gap is 10 times as large as the base case. $\gamma = 30$ represents a case of high left-digit bias where the discontinuity gap is 30 times as large as the base case.

Our simulation results are shown in Figure EC.6. With 10 arms, we observe that left-digit discontinuities do not affect GP-based algorithms. This outcome is expected: with only 10 prices tested, each price falls within a separate interval of the piecewise reward function, leaving sufficient distance between arms so the discontinuities have no impact. Of course, the GP estimates will not extrapolate well to other prices as it still assumes continuity (when it is in fact discontinuous at certain points), but the discontinuities will not affect the estimates at the test prices themselves. In both cases (low γ and high γ), the algorithm performs as well as in cases without left-digit discontinuities.

The issue arises when multiple prices are tested within each interval, requiring the GP to learn both the continuous segments and the discontinuous jumps. Because the GP assumes continuity, it tends to smooth over these jumps, resulting in slight misestimation of the demand curve. For instance, in the Beta(2,2) case across all four conditions (arms x γ), the price yielding the highest rewards is 0.39. For GP-TS-M, the performance decline from 10 to 100 arms (after 2500 consumers) is minor with low left-digit discontinuity gaps ($\gamma = 10$), dropping from 97.4% to 96.9%. However, with high left-digit discontinuity gaps ($\gamma = 30$), this decline is more pronounced, from 97.7% to 95.0%, as the GP smooths over a larger discontinuity and selects slightly sub-optimal prices (in subfigure d)ii) of Figure EC.6, the cumulative optimal rewards curve for GP-TS-M flattens before reaching the optimal, as the algorithm typically chooses 0.43, which provides 3% less reward than 0.39). Despite the GP's difficulty in handling discontinuities with 100 arms, the monotonic

Figure EC.6 Left Digit: Cumulative Percent of Optimal Rewards (Profits)

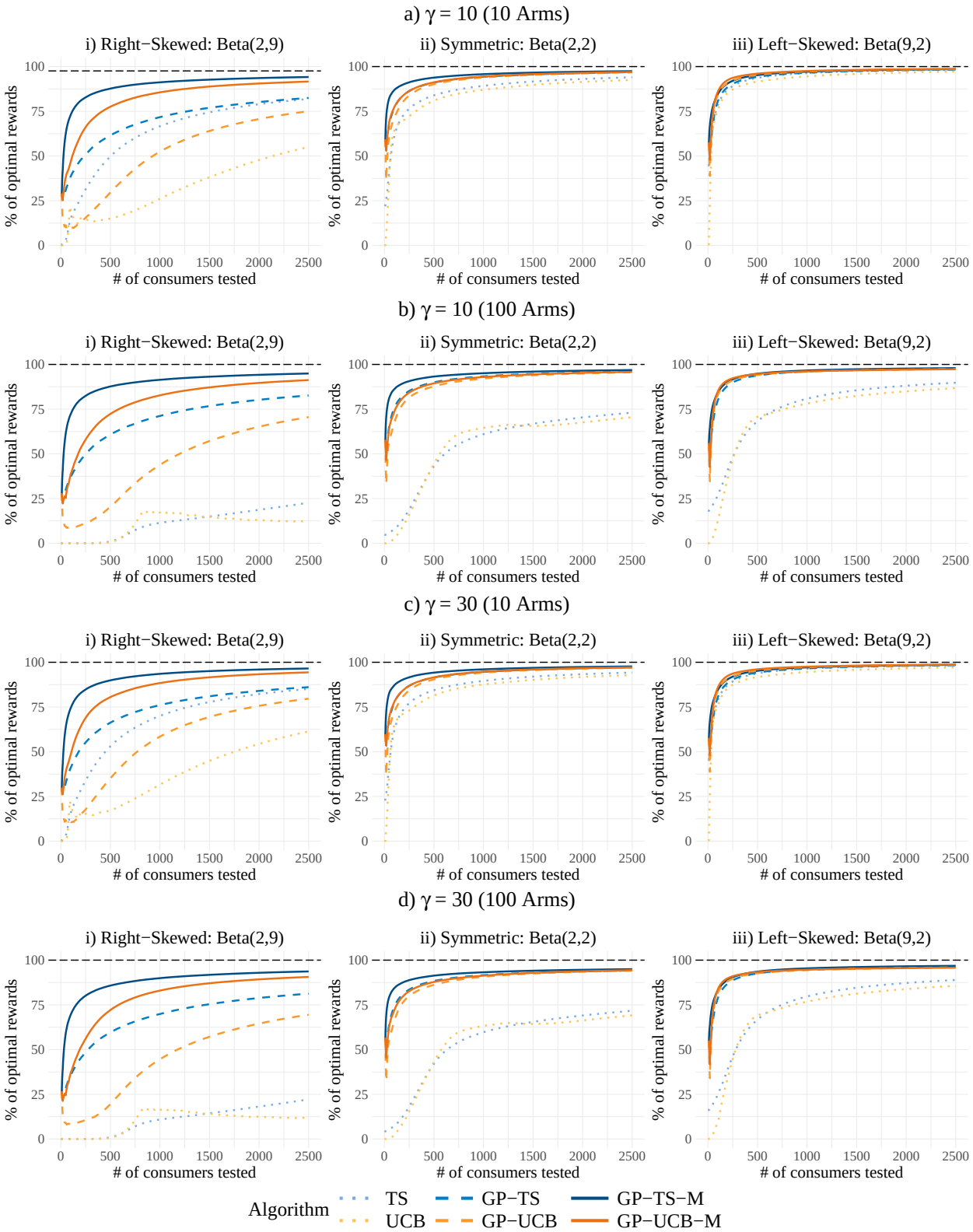

Notes. The lines are the means of the cumulative expected percentage of optimal rewards across the 1000 simulations. The black horizontal line represents the maximum obtainable given the price set, while 100% represents the true optimal given the underlying distribution. γ is a measure of the size of the discontinuity spike that occurs at locations where the left-digit changes.

versions of the algorithm remain the best performers after 2500 customers. While TS and UCB (which handle discontinuities by modeling each arm independently) would eventually learn the optimal and surpass the performance of GP-TS-M and GP-UCB-M, the additional exploration cost from forgoing the informational externalities greatly outweighs the small performance loss from slight misestimation for any reasonable consumer count.

To summarize, even with left-digit bias, our algorithms continue to perform best empirically. From a managerial perspective, if a firm suspects left-digit bias, a practical approach is to just test prices at the discontinuities themselves (e.g., 1.99, 2.99, etc.) to avoid misspecification issues with the GP. However, testing fewer prices may reduce rewards if the reward from the optimal price within the chosen price set is lower than the true optimal. Thus, selecting how many prices to test involves balancing the chance of a higher optimal reward against a potential misestimate due to left-digit bias. This trade-off is evident in our experiments: in the Beta(2,9) case, GP-TS-M performed better with more test prices when left-digit bias was low [subfigure a)i) vs. b)i)] but worse when left-digit bias was high [subfigure c)i) vs. d)i)].

EC.7 Time Varying Demand

We now consider the case where there are demand changes depending on the season (Soysal and Krishnamurthi 2012). We model the demand curve as undergoing a shift after every X consumers.[34] We denote the magnitude of the shift in the WTP distribution by δ, which results in a changed demand curve (shifted horizontally).

We explore the performance of the algorithms proposed in the paper, GP-TS and GP-TS-M, as well as their variants (GP-TS (Reset) and GP-TS-M (Reset)), which reset the learning process after every X consumers (seasonality cycle). The reset algorithm thus forgets all its history after every X periods, coinciding with shifts in the demand curve.

We observe that there are two separate effects that determine the effectiveness of the reset algorithm relative to the baseline ones. First, resetting is costly in terms of learning because the algorithm needs to re-learn the demand from the beginning (prior distribution). Second, on the flip side, resetting allows for more accurate learning when the underlying demand has changed. Thus, when δ is higher and the demand curve shifts are larger, it might be advantageous to reset, relative to GP-TS and GP-TS-M. The question of absolute

[34] The model can be extended to having a distribution for the number of consumers served, after which it undergoes a shift.

Figure EC.7 Time Varying: Cumulative Percent of Optimal Rewards (10 arms)

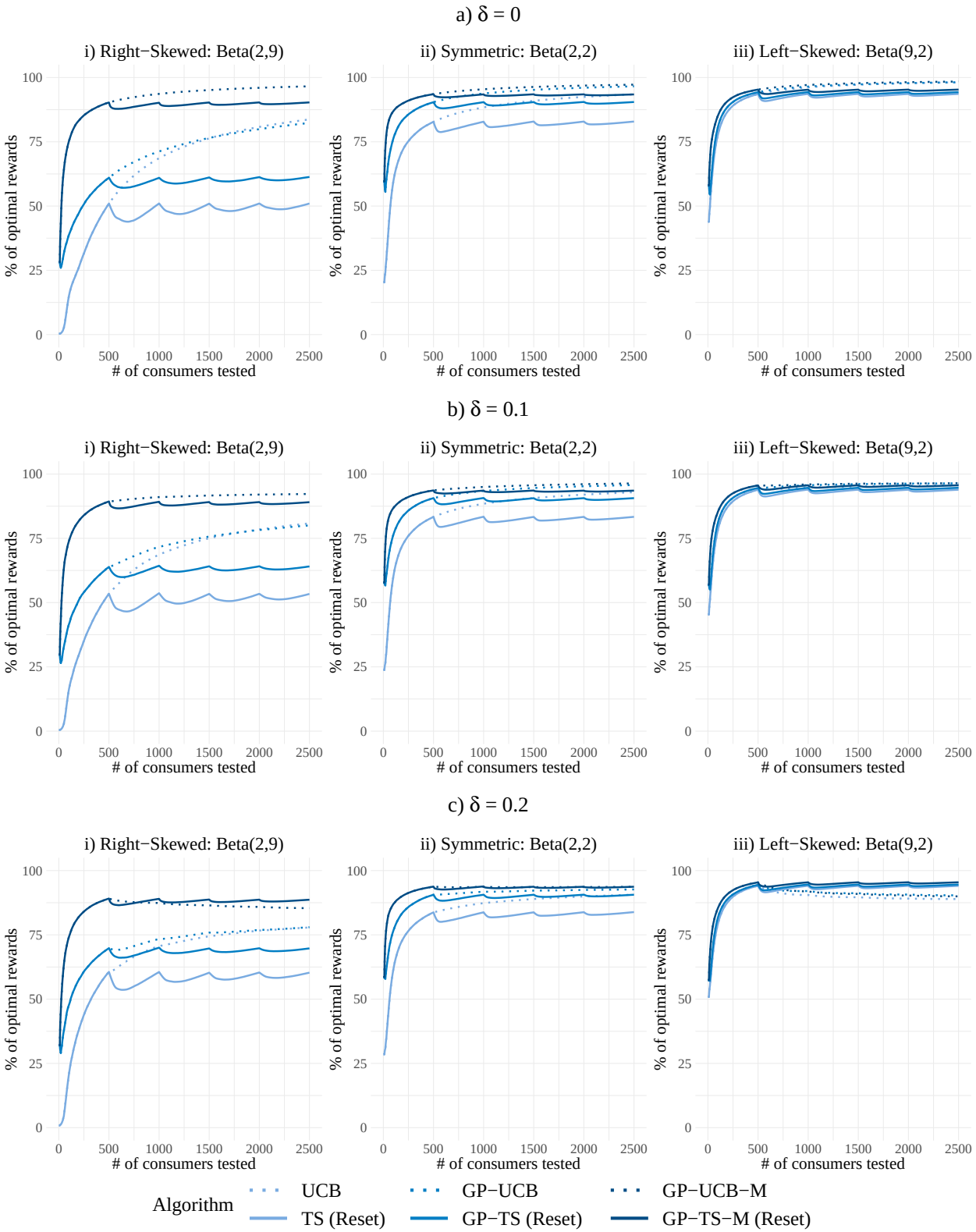

Notes. The lines are the means of the cumulative expected percentage of optimal rewards across the 1000 simulations. The black horizontal line represents the maximum obtainable given the price set, while 100% represents the true optimal given the underlying distribution. δ controls the size of the demand shock with a new time period starting every 500 consumers.

and relative performance of the two sets of algorithms (with and without reset) depends on the interplay of the above effects.

The results from the case with time varying demand are detailed in Figure EC.7. The previously explained baseline algorithms without reset are illustrated using dotted lines, whereas the new reset algorithms are illustrated by solid lines. When there is no underlying shift in the demand curve ($\delta = 0$), then it is obvious that resetting would always be worse in terms of performance, which is confirmed in the top row of panels. We observe that resetting can provide higher performance as the underlying shift increases to $\delta = 0.1$ and $\delta = 0.2$. We also see that the rank ordering of the algorithms within the reset (or non-reset) category is stable, and does not change with either the valuation distribution or the number of arms.

Observe that the left-skewed Beta(9, 2) distribution is relatively easy to learn the optimal, as the optimal price is high. In this case, we find that resetting does not result in a large cost, and the algorithm with resetting can do better for every algorithm with enough of an underlying shift ($\delta = 0.2$).

However, when the learning problem is relatively more challenging, with the Beta(2,9) or right-skewed distribution, we observe that resetting can result in a very high cost. In particular, resetting with TS and GP-TS performs quite poorly compared to no reset even with high time varying shifts ($\delta = 0.2$). However, if the learning process is quick enough (GP-TS-M), the value of resetting and learning the true optimal can be greater than the cost of re-learning. Thus, the value of adding informational externalities (especially the monotonicity constraint) results in a persistent advantage.

EC.8 Heteroscedastic Noise

One reason that GP-based algorithms can perform poorly is that the uncertainty (noise) parameter is set to be homoscedastic when the true underlying noise is actually heteroscedastic. For example, the sample mean at a price where nearly every single consumer purchases (or does not purchase) will be much less noisy than a price where consumers are equally likely to purchase and not purchase. For UCB and TS, heteroscedastic noise is not much of a problem, as they learn each arm independently. However, GP-TS shares information across arms, and while this is beneficial (especially with a large number of nearby arms), this also means that the noise is shared across arms, which is particularly problematic when the noise is modeled to be homoscedastic. This explains why we observe

in Table 4, in the case of five arms, that GP-TS performed worse than TS. When there is little to gain from sharing across arms (few arms that are far apart), the gain from sharing across arms is less than the negative caused by the misspecification of using homoscedastic noise. This appendix provides an alternative method of tuning the noise hyperparameter, which allows for heteroscedasticity. Empirically, this change is a complement to monotonicity and led to a small increase in algorithmic performance in every simulation setting tested.

While there are approaches to estimate a GP with heteroscedastic noise (Goldberg et al. 1997, Kersting et al. 2007), it succumbs to the same issue as estimating the noise using MLE as our homoscedastic specification. That is, it can be difficult to identify the shape and noise hyperparameters (Murray 2008), which is quite problematic for bandits where an insufficient noise estimate can lead to the algorithm getting stuck on sub-optimal arms.

Another approach would be to model the error by specifying some underlying structural process. In our case, the noise of the data can be modeled depending on how likely a consumer is to purchase. In general, we can write $\sigma_y^2 = g(D(p))$ for some unknown function g. However, noise depends on the underlying distribution which is completely unknown, making it unlikely that any suitable candidates for $g(\cdot)$ exist.

Implementation: Our estimation process for heteroscedastic noise works as follows. The first step is to estimate the GP using homoscedastic noise, which produces the results usually obtained. However, now we take a demand draw from this GP, which allows for the noise estimate to be calculated as the purchase decision is Bernoulli. A noise estimate can be calculated from the demand draw for each p in the test set as $\tilde{D}(p)(1-\tilde{D}(p))$. Another GP is then derived using this estimation as the noise input (tuning the shape hyperparameters per usual). We call the implementation *GP-TS-H*, reflecting the flexible heteroscedastic specification. This implementation can easily be merged with *GP-TS-M* by using monotonic draws to create *GP-TS-M-H*. Importantly, this method provides a way to provide better estimates of the noise without the algorithm getting stuck underestimating for a particular price.

The results are presented in Figure EC.8. They show that including heterogeneity on top of monotonicity leads to a small increase across all simulations. Like for the other informational externalities, the effects are the largest for the Beta(2,9) case. This is because smaller noise hyperparameters synergize with monotonicity in reducing the space of potential demand curves in the low reward high price region.

Figure EC.8 Heteroscedasticity: Cumulative Percent of Optimal Rewards (Profits)

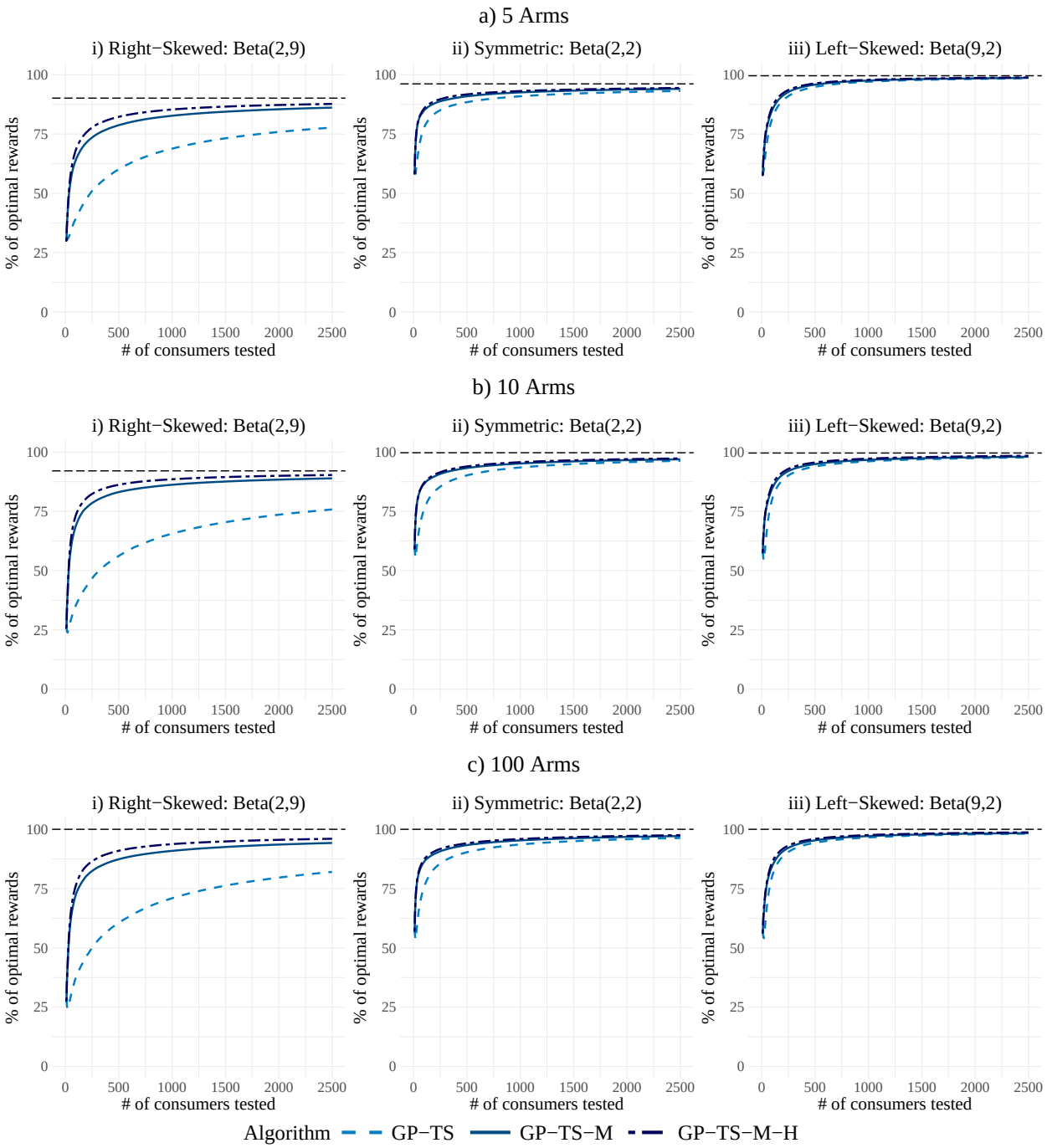

Notes. The lines are the means of the cumulative expected percentage of optimal rewards across the 1000 simulations. The black horizontal line represents the maximum obtainable given the price set, while 100% represents the true optimal given the underlying distribution.